Toxicology and Applied Pharmacology 302 (2016) 10–22

Contents lists available at ScienceDirect

Toxicology and Applied Pharmacology

journal homepage: www.elsevier.com/locate/ytaap

A semisynthetic diterpenoid lactone inhibits NF-κB signalling to ameliorate inflammation and airway hyperresponsiveness in a mouse asthma model

J.C.-W. Lim [a], F.-Y. Goh [b], S.-R. Sagineedu [c,1], A.C.-H. Yong [d,2], S.M. Sidik [e,3], N.H. Lajis [c], W.S.F. Wong [b,f,*], J. Stanslas [a,c,**]

[a] Pharmacotherapeutics Unit, Department of Medicine, Faculty of Medicine and Health Sciences, Universiti Putra Malaysia, 43400 Serdang, Selangor, Malaysia
[b] Department of Pharmacology, Yong Loo Lin School of Medicine, National University Health System, Singapore
[c] Laboratory of Natural Products, Institute of Bioscience, Universiti Putra Malaysia, 43400 Serdang, Selangor, Malaysia
[d] Faculty of Pharmacy, Segi University, Jalan Teknologi, 47810 Petaling Jaya, Malaysia
[e] Histopathology Unit, Department of Pathology, Faculty of Medicine and Health Sciences, Universiti Putra Malaysia, 43400 Serdang, Selangor, Malaysia
[f] Immunology Program, Life Science Institute, National University of Singapore, Singapore

ARTICLE INFO

Article history:
Received 8 October 2015
Revised 21 February 2016
Accepted 6 April 2016
Available online 27 April 2016

Keywords:
NF-κB
A549 cell line
Andrographolide analogues
Ovalbumin
Oxidative stress
Airway hyperresponsiveness
Mouse asthma model

ABSTRACT

Andrographolide (AGP) and 14-deoxy-11,12-didehydroandrographolide (DDAG), two main diterpenoid constituents of *Andrographis paniculata* were previously shown to ameliorate asthmatic symptoms in a mouse model. However, due to inadequacies of both compounds in terms of drug-likeness, DDAG analogues were semisynthesised for assessment of their anti-asthma activity. A selected analogue, 3,19-diacetyl-14-deoxy-11,12-didehydroandrographolide (SRS27), was tested for inhibitory activity of NF-κB activation in TNF-α-induced A549 cells and was subsequently evaluated in a mouse model of ovalbumin (OVA)-induced asthma. Female BALB/c mice, 6–8 weeks old were sensitized on days 0 and 14, and challenged on days 22, 23 and 24 with OVA. Compound or vehicle (3% dimethyl sulfoxide) was administered intraperitoneally 1 h before and 11 h after each OVA aerosol challenge. On day 25, pulmonary eosinophilia, airway hyperresponsiveness, mucus hypersecretion, inflammatory cytokines such as IL-4, -5 and -13 in BAL fluid, gene expression of inflammatory mediators such as 5-LOX, E-selectin, VCAM-1, CCL5, TNF-α, AMCase, Ym2, YKL-40, Muc5ac, CCL2 and iNOS in animal lung tissues, and serum IgE were determined. SRS27 at 30 μM was found to suppress NF-κB nuclear translocation in A549 cells. In the ovalbumin-induced mouse asthma model, SRS27 at 3 mg/kg displayed a substantial decrease in pulmonary eosinophilia, BAL fluid inflammatory cytokines level, serum IgE production, mucus hypersecretion and gene expression of inflammatory mediators in lung tissues. SRS27 is the first known DDAG analogue effective in ameliorating inflammation and airway hyperresponsiveness in the ovalbumin-induced mouse asthma model.
© 2016 Elsevier Inc. All rights reserved.

1. Introduction

Asthma is a chronic airway disorder characterised by airway inflammation, mucus hypersecretion, and airway hyperresponsiveness (AHR) (Kim et al., 2010). Cumulative evidence revealed that these inflammatory responses are mediated by T-helper type 2 (Th2) cells together with mast cells, B cells, and eosinophils by releasing various inflammatory cytokines and chemokines such as nitric oxide, histamine, IL-4, IL5, IL13, regulated upon activation normal T cell expressed and secreted (RANTES, CCL5) and Eotaxin (CCL11) (Lemanske and Jr Busse, 2003; Barnes, 2008). Th2 cytokines (IL-4, IL-5, and IL-13) and chemokines play pivotal roles in the pathogenesis of asthma. IL-4 is imperative for B cell isotype switching for the synthesis of IgE. Allergen-induced crosslinking of IgE-bound high-affinity IgE receptors (FcεRI) on the surface of mast cells leads to degranulation and activation of cells, release of inflammatory mediators like histamine, leukotrienes and cytokines, as

Abbreviations: (AGP), andrographolide; (AHR), airway hyperresponsiveness; (DDAG), 14-deoxy-11,12-didehydroandrographolide; (SRS27), 3,19-diacetyl-14-deoxy-11,12-didehydroandrographolide.

* Correspondence to: W.S.F. Wong, Department of Pharmacology, Yong Loo Lin School of Medicine, National University Health System, Singapore.
** Correspondence to: J. Stanslas, Pharmacotherapeutics Unit, Department of Medicine, Faculty of Medicine and Health Sciences, Universiti Putra Malaysia, 43400 Serdang, Selangor, Malaysia.
E-mail addresses: fred_wong@nuhs.edu.sg (W.S.F. Wong), rcxjs@upm.edu.my, jstanslas@yahoo.co.uk (J. Stanslas).
[1] Present address: International Medical University, No. 126, Jalan Jalil Perkasa 19, Bukit Jalil, 57000 Kuala Lumpur, Malaysia.
[2] Present address: MAHSA University, Lorong Dungun, 50490 Kuala Lumpur, Malaysia.
[3] Present address: Perdana University, Block B and D1, MAEPS Building, MARDI Complex, Jalan MAEPS Perdana, 43400 Serdang, Selangor, Malaysia.

http://dx.doi.org/10.1016/j.taap.2016.04.004
0041-008X/© 2016 Elsevier Inc. All rights reserved.

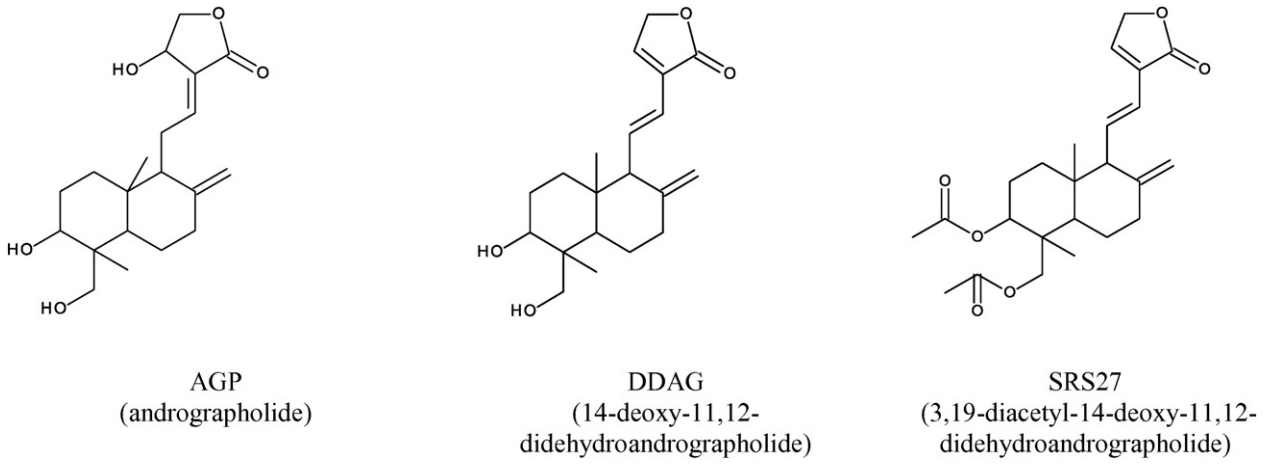


Fig. 1. Chemical structures of AGP, DDAG, SRS27, SRS28, SRS49, SRS76 and SRS83.

well as immediate bronchoconstriction (Galli et al., 2008). IL-5 is vital for the growth, differentiation, recruitment, and survival of eosinophils which contribute to inflammation and airway remodeling in asthma (Takatsu and Nakajima, 2008). IL-13 plays a critical role in the effector phase of Th2 responses such as eosinophilic inflammation, mucus hypersecretion, AHR and airway remodeling (Wills-Karp, 2004). In addition, chemokines such as CCL5 and CCL11 are crucial to the delivery of eosinophils to the airways (Hogan et al., 2008).

The clinical illness severity of asthma exacerbations is strongly associated with increased airway inflammation (Bartlett et al., 2012). In animal models, asthmatic inflammation had been linked with persistent NF-κB activation (Hart et al., 1998; Bureau et al., 2000; Bao et al., 2009; Barnes, 2011; Guan et al., 2011). Compared to control mice, the bronchial epithelium of mice sensitized and challenged with OVA exhibits robust and rapid inhibitory κB kinase α/β (IKK-α/β) activity and p65 nuclear translocation (Poynter et al., 2004). The Th2 responses in airway inflammation which leads to increase of Th2 cytokines level such as IL-4, IL-5 and IL-13 (Kato et al., 2007), and the chemokine CCL11 (Pope et al., 2005) in asthmatic inflammation is attributed to NF-κB p65 activation and nuclear translocation (Bartlett et al., 2012). As persistent NF-κB activation has been observed in all airway inflammations in both human and animal models of asthma (Barnes, 2011), various therapeutic strategies targeted at the NF-κB signalling pathway were attempted. NF-κB specific decoy oligonucleotide (Desmet et al., 2004), p65-specific antisense oligonucleotide (Choi et al., 2004), and IKKβ-selective small molecule inhibitor (Newton et al., 2007) have been demonstrated to possess beneficial effects in experimental asthma models. The anti-inflammatory effects of NF-κB decoy oligonucleotides had been reported in several preclinical studies for other inflammatory disease such as atopic dermatitis (De Stefano, 2011). However, systemic administration of these oligonucleotides is hampered by short half-life and non-specific distribution (De Stefano, 2011).

Andrographolide (AGP) and 14-deoxy-11,12-didehydroandrographolide (DDAG) are the main diterpenoid constituents from *Andrographis paniculata* (Lim et al., 2012). Studies have shown that both compounds inhibited airway inflammation in a mouse asthma model by targeting persistent NF-κB activity (Bao et al., 2009; Guan et al., 2011). In line with these findings, many of the AGP and DDAG analogues were also reported to possess potent anti-inflammatory activities (Lim et al., 2012). However, none of the semi-synthetic analogues have been reported to possess anti-inflammatory activities in experimental asthma models. A study conducted by Chao Chao et al. (2010) reported that acetylated AGP analogues strongly inhibit the effect on NF-κB-dependent nuclear trans-activation in the RAW 264.7 mouse macrophages. Interestingly, previous studies showed DDAG had reduced toxicity in several cell lines as compared to AGP (Guan et al., 2011). Therefore, SRS27 (Fig. 1), a derivative of DDAG with an acetyl group attached to each C3 and C19 of DDAG, was selected for further investigation of its anti-inflammatory activity in ovalbumin-induced asthmatic mouse model.

2. Methods

2.1. Isolation of AGP and DDAG, and synthesis of SRS27

AGP and DDAG were isolated and purified from *Andrographis paniculata* as reported previously (Fujita et al., 1984; Matsuda et al., 1994). For synthesis of SRS27, a mixture of DDAG (1 mmol) and acetic anhydride (50 mmol eq) was refluxed for 1 h. After completion of the reaction (checked by TLC), the reaction mixture was cooled to room temperature and diluted with water followed by extraction with

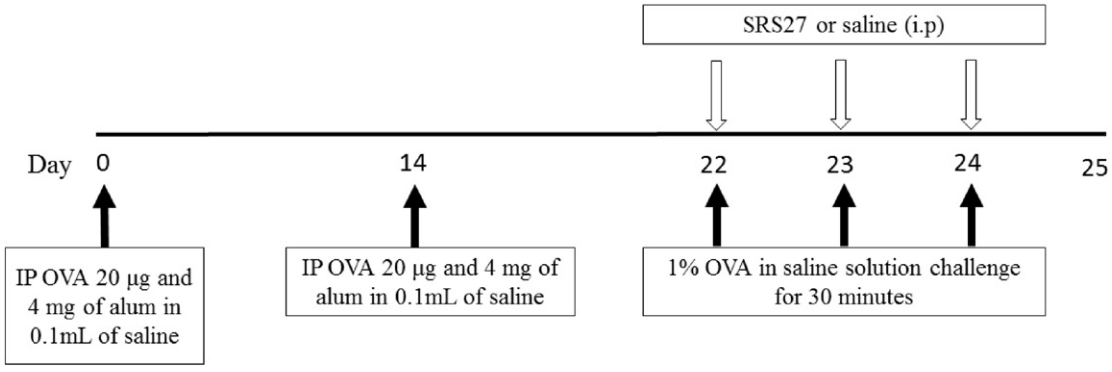
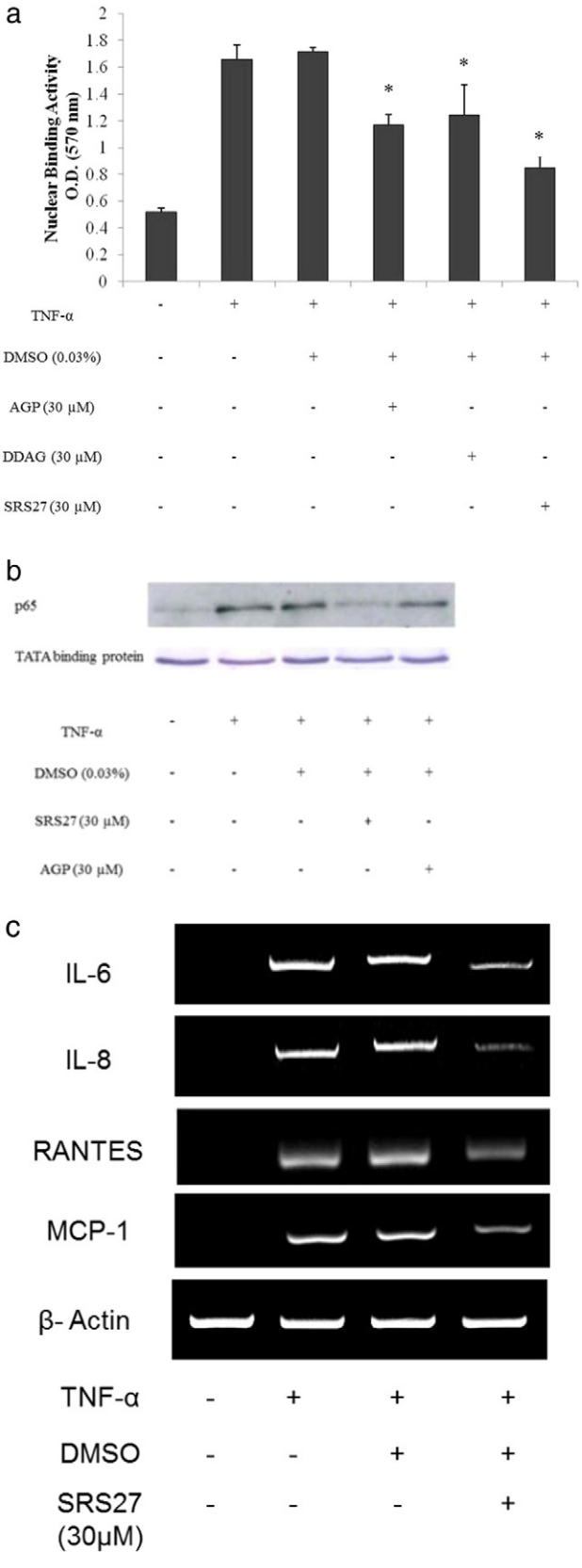


Fig. 2. Protocol of sensitization and treatment. The schedule of i.p. sensitization and treatment, and experiments are shown. Each group comprises of 7 mice. The procedures are described in materials and methods section.

dichloromethane. The organic layer was washed with brine, dried (over anhydrous Na_2SO_4), filtered and concentrated. The final residue was purified by centrifugal chromatography in a Chromatotron Model 7924 using silica gel 60 PF254 (Merck 7749) plates (2 mm thick) with dichloromethane–methanol (98:2) as an eluting solvent system. SRS27 was obtained as colorless solid (mp 102–104 °C; UV (solution in MeOH λ_{max}, nm) 208; IR (ATR) (ν_{max}, cm^{-1}): 2947, 2931, 1745, 1726, 1643, 1373, 1240, 893; MS (EI) *m/z*: 416 [M^+] (calculated for $C_{24}H_{32}O_6$, 416); ^1H NMR; ^{13}C NMR (Tables S3 and S4)).



2.2. Drug treatment and TNF-α stimulation in A549 cells

A549 cells were maintained in RPMI 1640 culture medium, supplemented with 10% heat-inactivated FBS, 100 U/mL of penicillin and 100 μg/mL of streptomycin. The cells were seeded onto 100 mm tissue culture dishes and 6-well plate 24 h before treated with 30 μM of SRS27 or vehicle (0.03% of DMSO) for 4 h. The cells were then stimulated with 10 ng/mL of TNF-α for 4 h for protein study and 12 h for gene expression study. Nuclear proteins were extracted for western blotting and NF-κB transcription factor assay whereas total mRNA was extracted for reverse transcriptase polymerase chain reaction (RT-PCR).

2.3. Immunoblotting, mRNA expression and NF-κB DNA-binding

Nuclear proteins of A549 cells or lung nuclear protein (10 μg per lane) were separated by 10% SDS-PAGE and immunoblots were developed as described (Goh et al., 2012). Immunoblots were probed with anti-p65 and anti-β-actin antibodies (all from Cell Signalling Technology, Beverly, MA), and anti-TATA binding protein (TBP, Abcam, Cambridge, UK). Primers for inflammatory biomarkers are shown in Table S1 and mRNA expression was analyzed as described (Goh et al., 2012). Nuclear proteins of A549 cells or lung nuclear protein were analyzed for NF-κB DNA-binding activity using the TransAM NF-κB p65 transcription factor kit (Active Motif, Carlsbad, CA).

2.4. In vitro cell viability assay

This assay was carried out as previously described (Jada et al., 2006). Cells were exposed to compounds (AGP, DDAG or SRS27) for 4 h followed by removal of compounds from the media. The cells were then incubated for 24, 48 and 72 h in compound free media at 37 °C in an atmosphere of 5% CO_2 and 95% air. Following that, 50 μL of MTT (2 mg/ml in PBS) was added into each well containing the cells in 200 μL medium and allowed for 4 h of incubation. The suspension of MTT and medium was then aspirated from each well and 100 μL of DMSO was added into each well. The absorbance of formazan was read at 550 nm using a microplate reader.

2.5. Animals

BALB/c mice were purchased from animal centre of National University Singapore and maintained in SPF facilities. Six- to eight-week-old female mice, with body weights of 16–20 g, were used in all experiments.

Fig. 3. Effects of SRS27 on TNF-α stimulation of A549 cells. (a) DNA-binding activity of p65 nuclear factor-kB in nucleus of A549 cells stimulated with TNF-α for 5 min in the presence or absence of 30 μM of test agents was determined using a TransAM p65 transcription factor ELISA kit. AGP, DDAG and SRS27 at 30 μM reduced nuclear binding activity. Nuclear binding activity is expressed as mean values ± SD (n = 3). (b) Representative images of immunoblotting of p65 level in nuclear extracts of A549 cells stimulated with TNF-α for 5 min in the presence and absence of 30 μM SRS27. TATA binding protein was used as a loading control. AGP and SRS27 significantly reduced NF-κB p65 level. (c) Representative gel images of polymerase chain reaction products of A549 cells stimulated with 10 ng/mL of TNF-α in the presence or absence of 30 μM SRS27 for 12 h (n = 3). β-Actin was used as an internal control. SRS27 at 30 μM markedly inhibited up-regulation of IL-6, IL-8, CCL2 and CCL5 in TNF-α activated A549 cells. All values shown are mean ± SEM of three separate experiments. *Significant difference from dimethyl sulfoxide control, $P < 0.05$.

2.6. Intraperitoneal treatment and sensitization

To examine the effect of SRS27 on the OVA immune response, mice (7 per group) were sensitized with OVA (200 μg/mL) in alum on day 0 and day 14. Mice were challenged with 1% OVA in saline solution for 30 min on days 22, 23, and day 24 as described in Fig. 2. SRS27 (0.1, 0.3, 1.0 and 3.0 mg/kg) or vehicle (3% dimethyl sulfoxide [DMSO]) in 0.1 mL of saline was administered intraperitoneally 1 h before and 11 h after each OVA aerosol challenge. Saline aerosol was used as a negative control. Ethical approval to conduct the animal experiments was obtained from the Animal Care and Use Committee of the National University of Singapore (IACUC/09/64).

2.7. Bronchoalveolar lavage fluid and serum analysis

Mice were anesthetized 24 h after the last aerosol challenge and bronchoalveolar lavage (BAL) was performed as described (Goh et al., 2012) on day 25 (Fig. 2). BAL fluid total and differential cell counts (Goh et al., 2012), and cytokine and chemokine levels (Goh et al., 2012; Ho et al., 2012) were determined as described (Goh et al., 2012) on day 25. Blood was collected by cardiac puncture, and serum levels of total IgE and OVA-specific IgE, IgG1, and IgG2a levels were determined as described (Goh et al., 2012) on day 25.

2.8. Histologic analysis

Lungs were fixed in 10% neutral formalin, paraffinized, cut into 5 μm sections, and stained with hematoxylin and eosin (H&E) for examining cell infiltration and with periodic acid-Schiff stain (PAFS) for measuring mucus production. In PAFS, sulfited acriflavine was bonded covalently with mucin glycoconjugate. On the other hand, acriflavine was binded in a non-covalent manner to the nucleic acid, nuclei, and cytoplasm. The mucin granules emitted red fluorescence and the other components of the cells emitted green fluorescence when excited at 390–580 nm and observed at 600–650 nm. The mucus was visualized using a confocal microscope (Leica TCS SP5, Leica Microsystems, Deerfield, IL, USA). Quantitative analysis of inflammatory cell infiltration and mucus production was performed blinded as described (Goh et al., 2012).

2.9. Measurements of airway hyperresponsiveness

Mice were anesthetized and tracheotomy was performed as described (Goh et al., 2012). The internal jugular vein was cannulated and connected to a microsyringe for intravenous methacholine administration. Airway resistance (Rl) and dynamic compliance (Cdyn) in response to increasing concentrations of methacholine were recorded using a whole-body plethysmograph chamber (Buxco, Sharon, CT) as

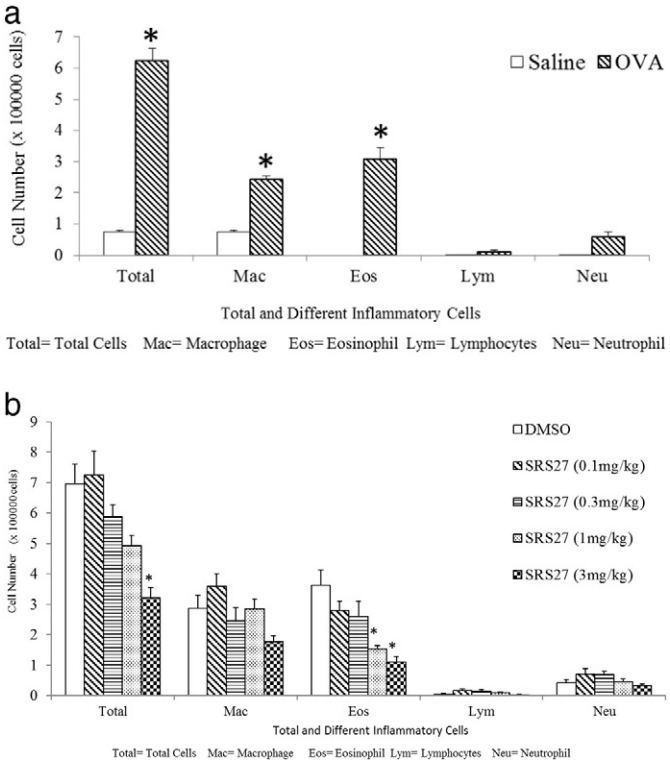


Fig. 4. Effects of SRS27 on ovalbumin (OVA)-induced inflammatory cells recruitment and mucus hypersecretion. (a) Total and different inflammatory cell counts in BAL fluid of OVA-sensitized and saline-challenged (Saline) and OVA-sensitized and OVA-challenged (OVA) mice. In saline-challenged mice, almost all cells observed in the BAL fluid under microscopic examination were macrophages, with few or no eosinophils, lymphocytes and neutrophils. OVA-challenged mice had significantly ($P < 0.05$) increased cell counts for total cells, macrophages and eosinophils. Values are expressed as mean ± SD (n = 7). *Significantly different from saline control ($P < 0.05$). (b) Total and differential cell counts were performed on BAL fluid obtained from vehicle control (3% DMSO) mice, and four drug treatment groups (0.1, 0.3, 1.0 and 3.0 mg/kg SRS27) 24 h after the last aerosol challenge. SRS27 at 0.1 mg/kg, 0.3 mg/kg, 1.0 mg/kg and 3.0 mg/kg decreased the total cell count as well as the number of macrophages, eosinophils, neutrophils and lymphocytes in BAL fluid in a dose-dependent manner as compared with the DMSO vehicle control. Values are expressed as mean ± SD (n = 7). *Significantly different from saline control ($P < 0.05$). (c) Representative photomicrographs of lung sections of saline control mice, OVA-challenged mice, OVA-challenged and DMSO-treated mice, and OVA-challenged and 3.0 mg/kg SRS27-treated mice 24 h after the last aerosol challenge. SRS27 significantly reduced inflammatory cells infiltration as compared to DMSO control. Hematoxylin and eosin stain × 400. Values shown are the mean ± SD (n = 3). *Significantly different from vehicle control (3% DMSO), $P < 0.05$. Quantitative analyses of inflammatory cell infiltration in lung sections were performed as previously described (Goto et al., 2009). (d) Representative fluorescent photomicrographs of saline control mice, OVA-challenged mice, OVA-challenged and DMSO-treated mice, and OVA-challenged and 3.0 mg/kg SRS27-treated mice 24 h after the last aerosol challenge. Note that mice treated with SRS27 24 h after the last aerosol challenge significantly reduced mucus hypersecretion as compared to DMSO control. Periodic acid–Schiff stain × 1000. Values shown are the mean ± SD (n = 3). *Significantly different from vehicle control (3% DMSO), $P < 0.05$. Quantitative analyses of mucus production in lung sections were performed as previously described (Goto et al., 2009).

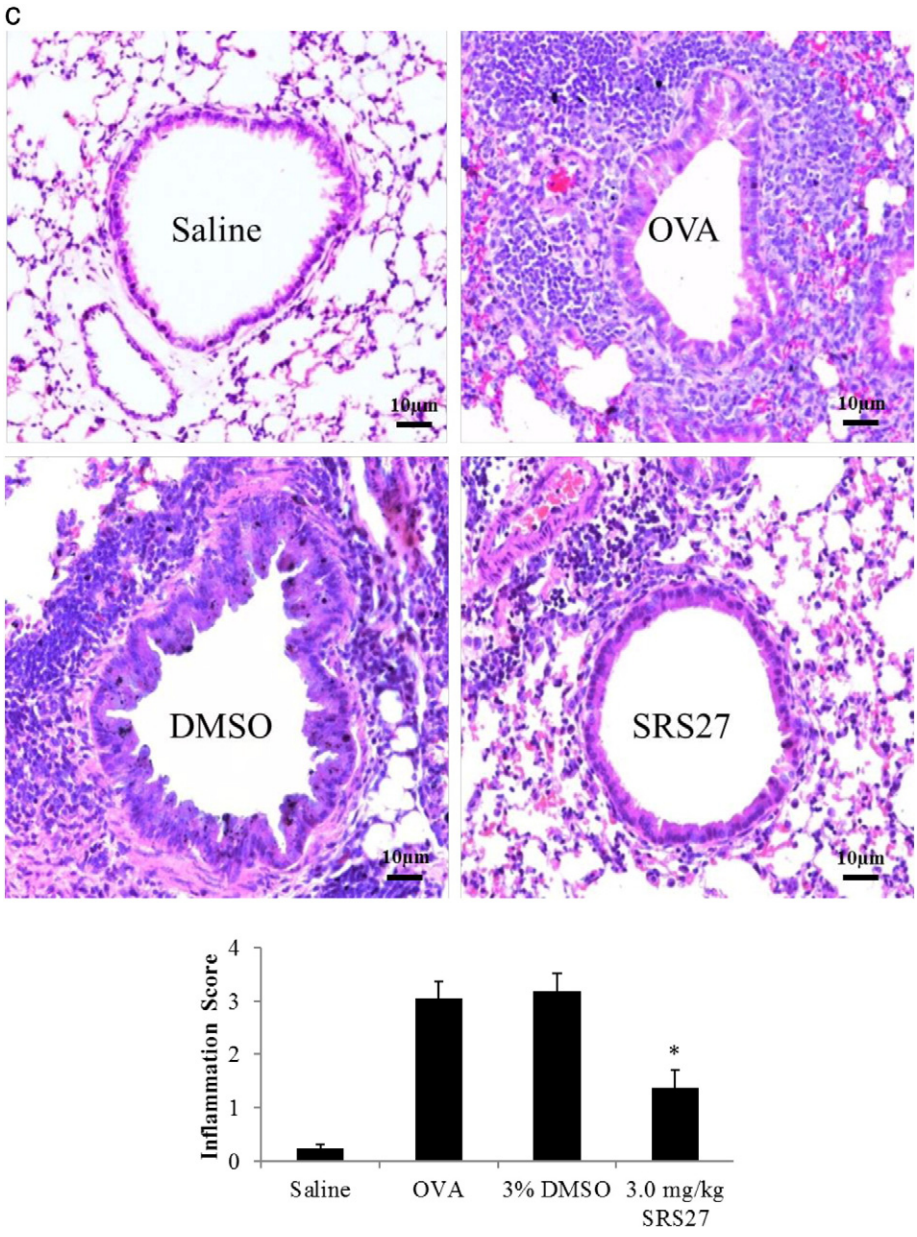


Fig. 4 (*continued*).

described (Goh et al., 2012). Results were expressed as a percentage of the respective basal values in response to phosphate-buffered saline.

2.10. Statistical analysis

Data are presented as means ± SEM. One-way analysis of variance (ANOVA) followed by Dunnett test was used to determine the significant differences between treatment groups. Significant levels were set at $P < 0.05$.

3. Results

3.1. SRS27 inhibits NF-κB activation

TNF-α plays a critical role in asthma (Brightling et al., 2008; Vroling et al., 2007) and is a potent stimulator of human airway epithelial cells (Newton et al., 2007). To investigate whether SRS27 possesses anti-inflammatory activity in a relevant airway cell type, we first studied the effects of SRS27 on TNF-α-induced activation of NF-κB and cytokine mRNA expression in A549 cells. TNF-α induced a sharp increase of p65 level in the nucleus and p65 DNA-binding activity (Fig. 3a and b) and SRS27 markedly ablated the nuclear translocation of p65 subunit of NF-κB and DNA binding in nucleus (Fig. 3a and b). Furthermore, SRS27 significantly suppressed TNF-α-induced up-regulation of NF-κB dependent gene expression such as IL-6, IL-8, CCL5 and monocytes chemotactic protein (MCP)-1 (Fig. 3c).

3.2. SRS27 suppresses OVA-induced inflammatory cell recruitment and mucus production

BAL fluid was collected 24 h after the last OVA or saline aerosol challenge. Total and differential cell counts were performed. OVA inhalation markedly increased total cell, macrophage and eosinophils counts, but slightly increased lymphocyte and neutrophil counts, as compared with saline aerosol control (Fig. 4a). SRS27 (0.1, 0.3, 1 and 3 mg/kg) drastically decreased the total cell and eosinophil counts in BAL fluid in a dose-dependent manner as compared with the DMSO vehicle control (Fig. 4b). At the highest dose (3 mg/kg), SRS27 also reduced

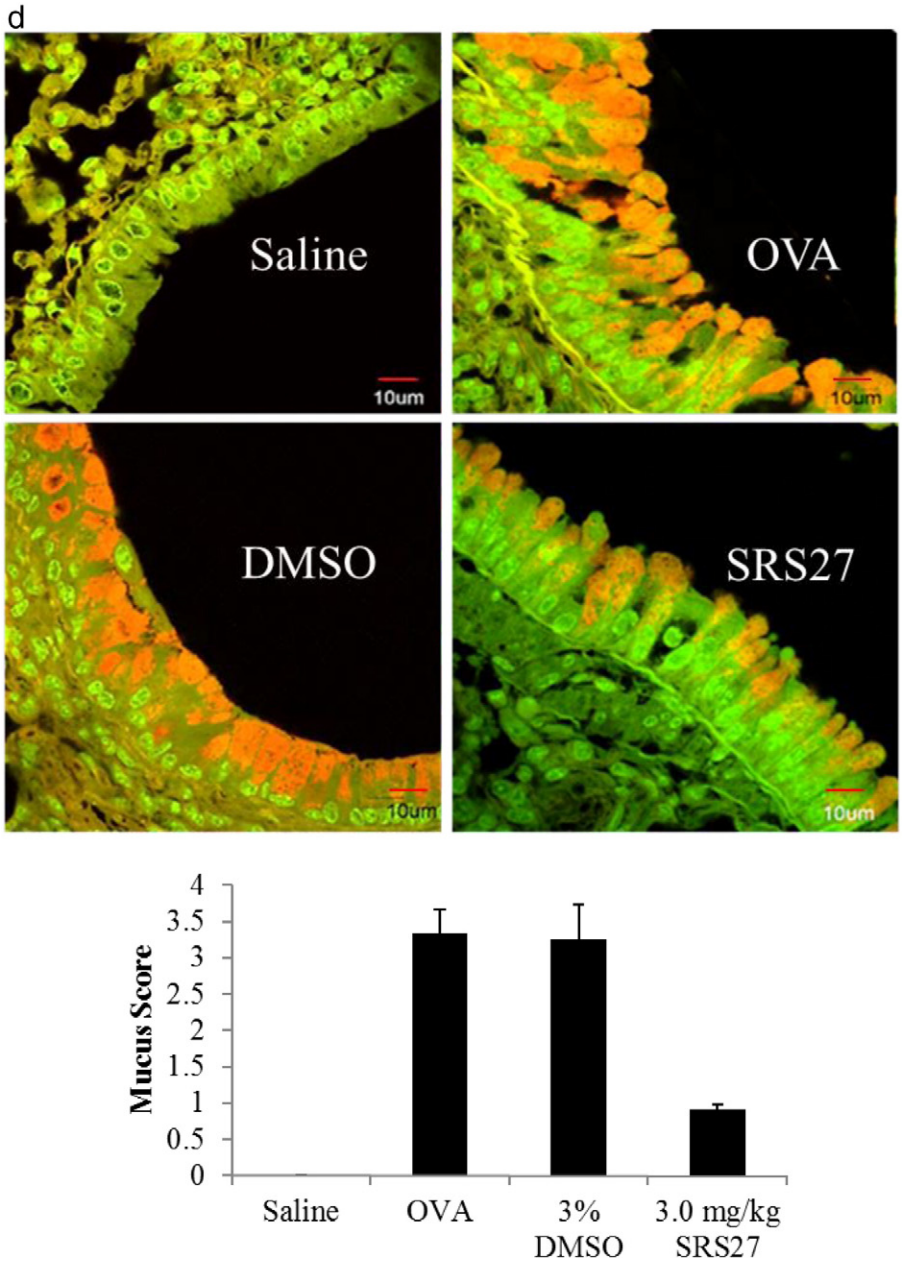


Fig. 4 (*continued*).

macrophage, lymphocyte, and neutrophil counts. Flow cytometric analysis of peripheral blood leukocytes obtained from saline-challenged, OVA-challenged, vehicle control, and SRS27-treated mice was conducted. Similar cell counts of total white blood cells, neutrophils, lymphocytes, monocytes, eosinophils, and basophils were observed in all mice (Fig. S2). Creatinine, aspartate transaminase (AST) and alanine transaminase (ALT) levels in serum of saline-challenged, vehicle control, and SRS27-treated mice indicated the compound did not adversely affect both kidney and liver function (Figs. S3 and S4). Besides, the percentage of normalised body weight changes relative to day 0 of saline-challenged, vehicle control, and SRS27-treated (3 mg/kg) indicated absence of toxicity in compound-treated group (Fig. S5). Hence, SRS27-induced reductions of eosinophil and lymphocyte pulmonary recruitment are unlikely due to any potential nonspecific cytotoxic effects of the compound. Lung tissues were also collected 24 h after last OVA or saline aerosol challenge. OVA aerosol challenge induced marked infiltration of inflammatory cells into the peribronchiolar and perivascular connective tissues as compared with saline aerosol challenge. SRS27 (3 mg/kg) reduced eosinophil-rich leukocyte infiltration as compared with DMSO control (Fig. 4c). On the other hand, OVA challenged mice developed marked goblet cell hyperplasia and mucus hypersecretion in the bronchi. OVA-induced mucus hypersecretion was significantly halted by SRS27 (3 mg/kg) (Fig. 4d).

3.3. SRS27 reduces OVA-induced bronchoalveolar lavage fluid T helper type 2 cytokine levels and serum immunoglobulin production

OVA inhalation in sensitized mice caused a notable increase in IL-4, IL-5, IL-13, and CCL11 levels into BAL fluid as compared with saline aerosol control (Fig. 5a, b, c and d). In contrast, BAL fluid level of IFN-γ, a Th1 cytokine, dropped slightly in OVA challenged mice (Fig. 5e). SRS27 significantly ($P < 0.05$) reduced IL-4, IL-5, and IL-13 and, to a lesser extent, CCL11 levels in BAL fluid in a dose-dependent manner as compared with DMSO control (Fig. 5a, b, c and d). Noticeably, SRS27 at 3 mg/kg markedly up-regulated IFN-γ level in BAL fluid (Fig. 5e). The gene expression of IL-33, which is a strong inducer of Th2 immune responses, was

significantly up-regulated in OVA aerosol challenged mice and significantly down-regulated by SRS27. These findings imply that SRS27 is capable of modifying Th2 predominant immune activity in an OVA-mouse model of asthma. To further evaluate whether SRS27 could modify an ongoing OVA-specific Th2 response *in vivo*, serum levels of total IgE and OVA-specific IgE were determined using ELISA. Marked elevation in serum total IgE and OVA-specific IgE were observed in OVA-challenged mice as compared with saline-challenged mice (Fig. 5h and i). SRS27 strongly suppressed OVA-specific IgE and total IgE levels even at low dose (0.3 mg/kg), and to a lesser extent, the serum level of total IgE with significant effects at higher dose (3 mg/kg) (Fig. 5h and i).

3.4. SRS27 ameliorates OVA-induced oxidative lung damage

To determine the level of OVA-induced oxidative lung damage, 8-OHdG and 8-isoprostane levels in BAL fluid were measured using ELISA. 8-OHdG is a marker for oxidative DNA damage (Giustarini et al., 2009a); while 8-isoprostane is an indicator for lipid peroxidation (Wood et al., 2003). OVA aerosol exposure greatly enhanced 8-OHdG levels in the BAL fluid by approximately four folds, in comparison to saline aerosol control (Fig. 5g). SRS27 at 1 and 3 mg/kg significantly blocked oxidative DNA damage by suppression of 8-OHdG levels in a dose-dependent manner. One fold increase of 8-isoprostane level in BAL fluid was observed upon OVA challenge (Fig. 5f). Results suggest that SRS27 dose-dependently reduced oxidative damage to lipids by decreasing 8-isoprostane formation compared to saline aerosol control. To further verify the level of oxidative lung damage, gene expression of oxidative stress markers (SOD-2 and catalase) in lung tissues were measured. OVA aerosol challenge strongly up-regulated SOD-2 and down-regulated catalase gene expression. Pre-treatment of SRS27 significantly reduced SOD-2 and increased catalase gene expression (Fig. 7a).

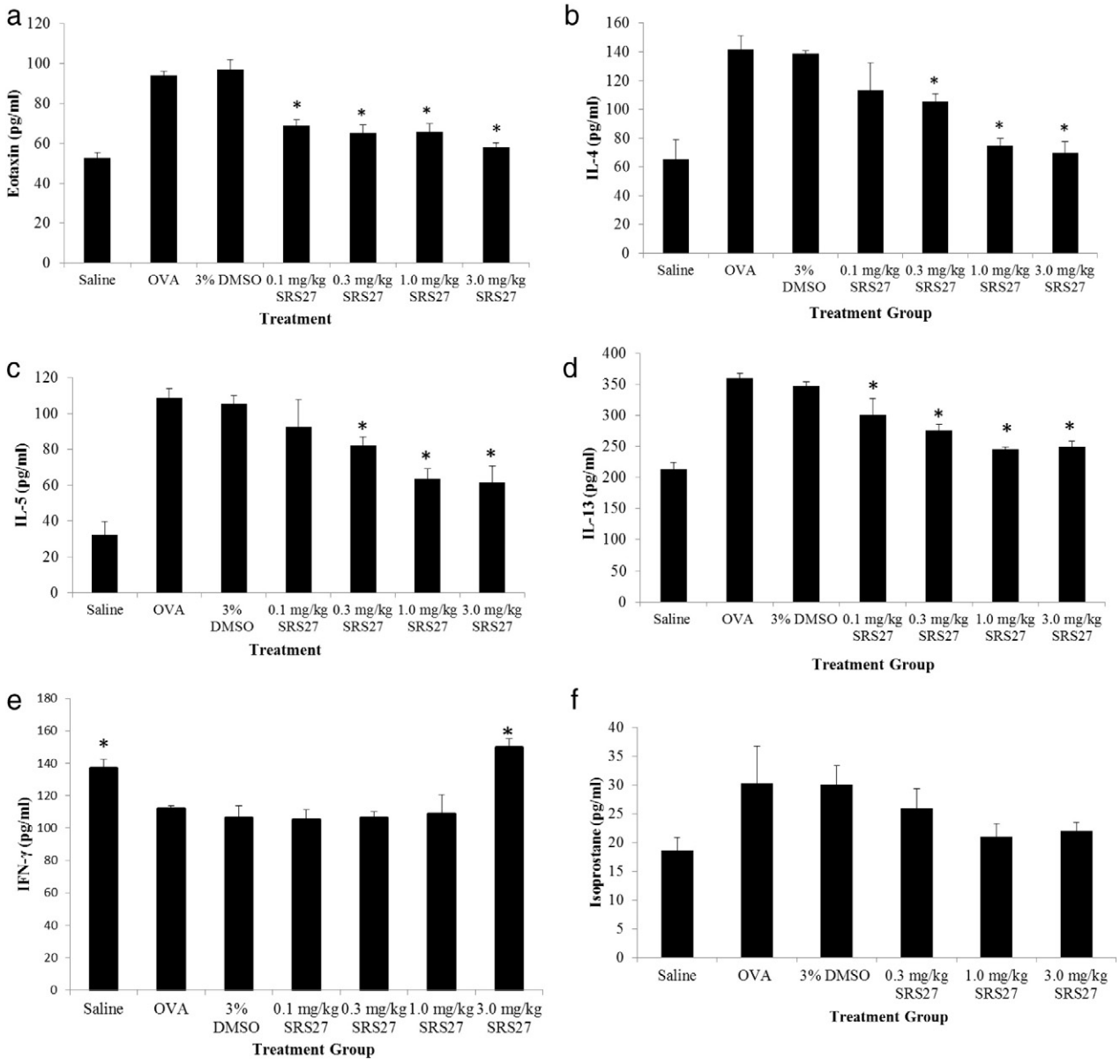


Fig. 5. Levels of CCL11 (a), IL-4 (b), IL-5 (c), IL-13 (d), IFN-gamma (e), isoprostane (f), and 8-OH-2-deoxyguonosine (g) in BAL fluid and levels of OVA-IgE (h) and total IgE (i) in serum of Saline = saline control mice, OVA = OVA-challenged mice, 3% DMSO = DMSO-treated mice, and SRS27 = 0.1, 0.3, 1.0, and 3.0 mg/kg SRS27-treated mice measured using enzyme-linked immunosorbent assay (ELISA). SRS27 dose-dependently reduced CCL11, IL-4, IL-5, IL-13, isoprostane and 8-OH-2-deoxyguonosine level in BAL and OVA-IgE and total IgE in serum. SRS27 markedly increased IFN-γ level at 3.0 mg/kg against OVA and DMSO controls. Values shown are the mean ± SEM (n = 5). *Significant difference from 3% DMSO in saline control, $P < 0.05$.

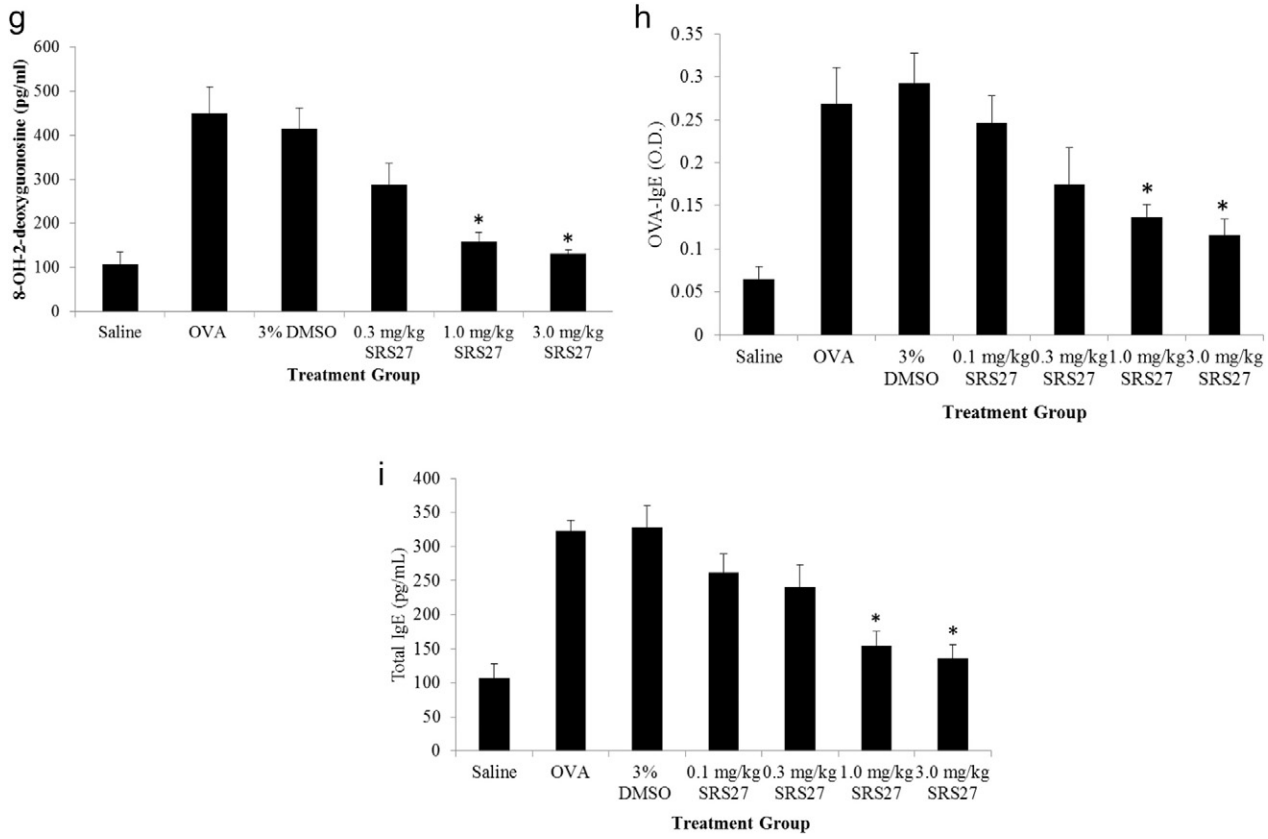


Fig. 5 (*continued*).

3.5. SRS27 reduces OVA-induced airway hyperresponsiveness in mice

To investigate the effect of SRS27 on AHR in response to increasing concentrations of methacholine, we measured Rl and Cdyn in mechanically ventilated mice. Rl is defined as the pressure driving respiration divided by flow. Cdyn refers to the distensibility of the lung and is defined as the change in volume of the lung produced by a change in pressure across the lung. OVA-challenged mice developed AHR, which was typically reflected by high Rl and low Cdyn (Fig. 6). SRS27 (3 mg/kg) dramatically reduced Rl and restored Cdyn in OVA-challenged mice in response to increased methacholine dosing, suggesting that immune-mediated airway pathology *in vivo* was modified.

3.6. SRS27 inhibits OVA-induced NF-κB function and inflammatory gene expression in airway inflammation

OVA aerosol challenge marked up-regulated lung mRNA levels of 5-Lipoxygenase (5-LOX) which is an arachidonic acid metabolic enzyme that is responsible for synthesis of leukotrienes (CysLT); adhesion molecule, E-selectin and VCAM-1, which are pivotal for pulmonary recruitment of inflammatory cells, such as eosinophils and lymphocytes; chemokine molecule, CCL5 for active role in recruiting leukocytes into inflammatory sites; TNF-α, a potent NF-κB signalling inducer cytokine; chitinase family members, including acidic mammalian chitinase (AMCase), Ym2, and YKL-40, which have been shown to play critical roles in airway inflammation and remodeling; Muc5ac, which is essential for mucus hypersecretion; MCP-1(CCL2), a macrophage chemotactic protein; and iNOS. Pretreatment with SRS27 (3 mg/kg) demonstrated strong suppression of 5-LOX, E-selectin, VCAM-1, CCL5, TNF-α, AMCase, Ym2, YKL-40, Muc5ac, CCL2 and iNOS in asthmatic airways (Fig. 7a). To verify that the anti-inflammatory effects of SRS27 in OVA-challenged mice were mediated by the inhibition of NF-κB, as observed in our *in vitro* study (Fig. 3b and c), we examined the effect of SRS27 on nuclear translocation of NF-κB p65 sub-unit and p65 DNA-binding activity in lung tissues obtained 24 h after last OVA challenge or saline challenge were examined. OVA challenge markedly raised level of p65 subunit in the nuclear extract of the lung tissues and promoted nuclear p65 DNA-binding activity as compared with saline aerosol control (Fig. 7b and c). SRS27 (3 mg/kg) significantly ($P < 0.05$) reduced both nuclear p65 amount and DNA-binding activity to basal level (Fig. 7b and c), suggesting that SRS27 exert its anti-inflammatory actions *via* inhibition of NF-κB activity.

4. Discussion

AGP has been reported to be a good pharmacophore with diverse pharmacological activities. Esterification of either one or more of the three hydroxyls of AGP with short/long chains, heterocyclic, aromatic fatty acids was attempted and tested for a variety of activities. Most of the acetylated derivatives of AGP showed improved activity profiles especially anti-inflammatory property (Chao et al., 2010; Aromdee, 2012). Chao et al. (2010) reported that 3,19-*O*-diacetylanhydroandrographolide and 19-*O*-acetylanhydroandrographolide, strongly inhibit NF-κB-dependent transactivation in the RAW 264.7 cells, providing the support of using SRS27 in our study. Although AGP attenuates airway inflammation in an OVA-mouse model of asthma, it is a more toxic to cell lines than DDAG (Guan et al., 2011). This profile renders AGP as a less favorable compound to be developed as an anti-asthma drug. Hence, we believe that chemical modifications of DDAG could result in compound with better safety profile. SRS27, was synthesised by coupling two acetyl group to each C3 and C19 of DDAG. To verify that SRS27 is a compound as safe as DDAG, the toxicity effect of AGP, DDAG and SRS27 was evaluated in multiple cell lines. Results indicated that SRS27 had mild cytotoxic effect like DDAG, but lower compared with AGP (Fig. S1a–c). In animal model, the percentage of body weight

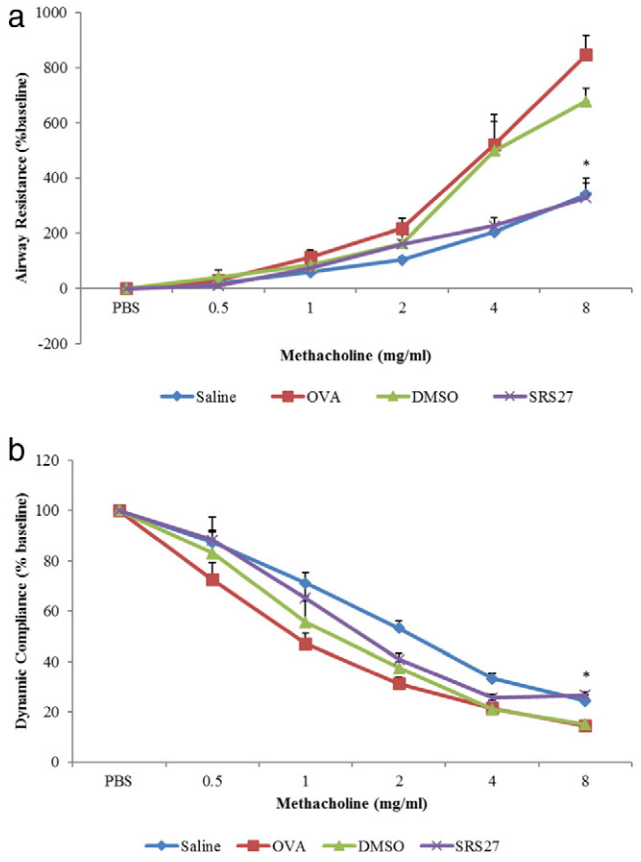


Fig. 6. Airway resistance (a) and dynamic compliance (b) of mechanically ventilated mice (Saline = saline control mice, OVA = OVA-challenged mice, 3% DMSO = DMSO-treated mice and SRS27 = 3.0 mg/kg SRS27-treated mice) in response to increasing concentrations of methacholine (0.5, 1.0, 2.0, 4.0 and 8.0 mg/kg). SRS27 at 3 mg/kg dramatically suppressed airway resistance and restored dynamic compliance to almost the basal levels of the saline control. Values shown are the mean ± SD (n = 7). *Significant difference from 3% DMSO in saline control, $P < 0.05$.

of mice against day 0 indicated that SRS27 exerted no toxic effects in the *in vivo* model (Fig. S5). This is supported by the level of AST, ALT and creatinine in serum of the *in vivo* model which indicated absence of toxicity towards kidney and liver function (Figs. S3 and S4).

Asthmatic inflammation has been closely associated with up-regulation of NF-κB activity in lung cells in human and animal models (Hart et al., 1998; Bureau et al., 2000; Bao et al., 2009). The ability of SRS27 to inhibit NF-κB activation by inhibiting nuclear translocation of p65 subunit of NF-κB and DNA binding activity leading to suppression the biological response associated with NF-κB activation (IL-6, IL-8, CCL2 and CCL5 gene expression) provided us with a the strong basis to evaluate SRS27 in the mouse model of asthma. Drugs which act primarily as NF-κB inhibitors are immunosuppressive, whereby they could inhibit beneficial immune responses even though the dose applied is safe in clinical applications (Gilmore and Herscovitch, 2006). Ciriaco et al. (2013), also raised concerns about the possibility of unwanted side effects of NF-κB inhibitor for treatment of inflammatory based diseases such as cancer and asthma. However, considering the broad spectrum of clinical indications, this class of drug has been reviewed as an important class of drug as long as the dose applied is safe in clinical application (Gilmore and Herscovitch, 2006). In asthma, activation of NF-κB occurs in localized site, within the airway of lung. To ensure SRS27 is safe in clinical application, the compound can be applied locally in the airway *via* an inhaler system or given orally in a low-dose to prevent the development of unwarranted side effects. As such, SRS27 still can be precluded its utility as a drug for asthma.

Drug development for asthma has been directed towards improving profile of currently available asthma drugs to discover new compounds that are able to target the Th2-driven airway inflammatory response (Caramori and Papi, 2004). The OVA-mouse model of asthma used in this study is mediated by Th2 immune response (Bao et al., 2009; Guan et al., 2011). Our present data show that SRS27 significantly reduced the level of IL-4, IL-5, IL-13, and CCL11 in BAL fluids form OVA-challenged mice. Repression of NF-κB signalling pathway has been shown to block IL-13-induced CCL11 production in cultured human airway smooth muscle cells (Goto et al., 2009). Our findings also revealed a significant inhibition of p65 nuclear translocation and NF-κB DNA binding activity by SRS27 in OVA-challenged lungs *in vivo*. Hence, we believe that SRS27 can effectively suppress various aspects of OVA-induced Th2 mediated airway inflammation in mice *via* inhibition of NF-κB activity at the p65 translocation level. Therefore, the observed reduction of IL-4, IL-5, IL-13, and CCL11 levels in BAL fluid from SRS27-treated mice may be due to the inhibition of NF-κB activation in the inflammatory and airway resident cells.

Our findings showed that SRS27 prevented inflammatory cell infiltration into the airway as evident by the significant decrease in total cell counts and eosinophil counts in BAL fluid, and in tissue eosinophilia in lung sections. Leukocyte transmigration into airways is orchestrated by cytokines, such as IL-4, IL-5, and IL-13, and coordinated by specific chemokines, such as CCL11 and CCL5, in combination with adhesion molecules, such as VCAM-1 and E-selectin (Barnes, 2011). We have demonstrated that SRS27 strongly suppressed E-selectin and CCL5, TNF-α mRNA expression and CCL11 production in OVA-challenged lungs. These findings are likely to be due to SRS27-mediated NF-κB inhibition, as the genes for E-selectin, CCL11, CCL5, TNF-α, and CCL11 contain the κB site for binding of NF-κB within their promoters (Schindler and Baichwal, 1994; Collart et al., 1990; Moriuchi et al., 1997; Hein et al., 1997). Taken together, the observed reduction in airway eosinophilia by SRS27 may be a result of combined inhibitory effects on IL-13, CCL11, and CCL5 production, and on E-selectin expression, secondary to inhibition of NF-κB activation.

We have also demonstrated a reduction in airway mucus production in SRS27-treated mice as compared with vehicle (3% DMSO) control. It was reported that 1% DMSO augmented IL-1β secretion in a dose- and time-dependent manner without altering TNF-α or IL-6 in LPS treated human PBMC and *in vivo* (Xing and Remick, 2005). Our study utilized DMSO as our cosolvent to dissolve SRS27 which was difficult to solubilize in saline alone. As DMSO has been reported with potential anti-inflammatory effects by up-regulating IL-1β secretion, concerns had been raised over the potential therapeutic effects by DMSO in our study. To address the raised concerns, vehicle control had been accounted for possible therapeutic effects by DMSO. Our *in vitro* and *in vivo* data had clearly highlighted that vehicle control played no role in therapeutic effects possibly due to increase of IL-6 and TNF-α level in both *in vitro* and *in vivo* findings. However, it remains possible that SRS27 and DMSO could exhibit additive or synergistic anti-inflammatory effect. Therefore, the use of alternative co-solvent without anti-inflammatory activity should be considered in the future studies.

Cumulative evidence indicates that IL-13 plays a critical role in goblet cell hyperplasia as well as mucin Muc5ac gene and protein expression in mice (Barnes, 2011). Our study showed that pretreatment of SRS27 in mice resulted in reduced BAL IL-13. This reduction is accompanied by significant reductions in 5-LOX and Muc5ac gene expression in lung tissues. In addition, NF-κB-dependent gene expression profiling of Hodgkin's disease tumor cells revealed that IL-13 gene expression is controlled and activated by NF-κB (Heinz et al., 2002). As such, the marked decrease in mucus production in the lungs of SRS27-treated mice may be attributable to a significant reduction of IL-13, which is mediated by a direct inhibitory action on NF-κB signalling pathway in airway epithelium.

Our data showed that serum levels of total IgE and OVA-specific IgE in serum were substantially reduced by SRS27 in OVA-challenged mice. Studies demonstrate that NF-κB plays a crucial role in B-cell proliferation

and development, hence IgE production (Schulze-Luehrmann and Ghosh, 2006; Matsumoto et al., 2006). Th2 cytokines (IL-4 and IL-13) are important in directing B-cell growth, differentiation, and secretion of IgE (Wills-Karp, 2004; Li-Weber and Krammer, 2003). The biological activities of IgE are mediated through its interaction with the FcεRI on the mast cells and basophils. Cross-linking of FcεRI initiates multiple

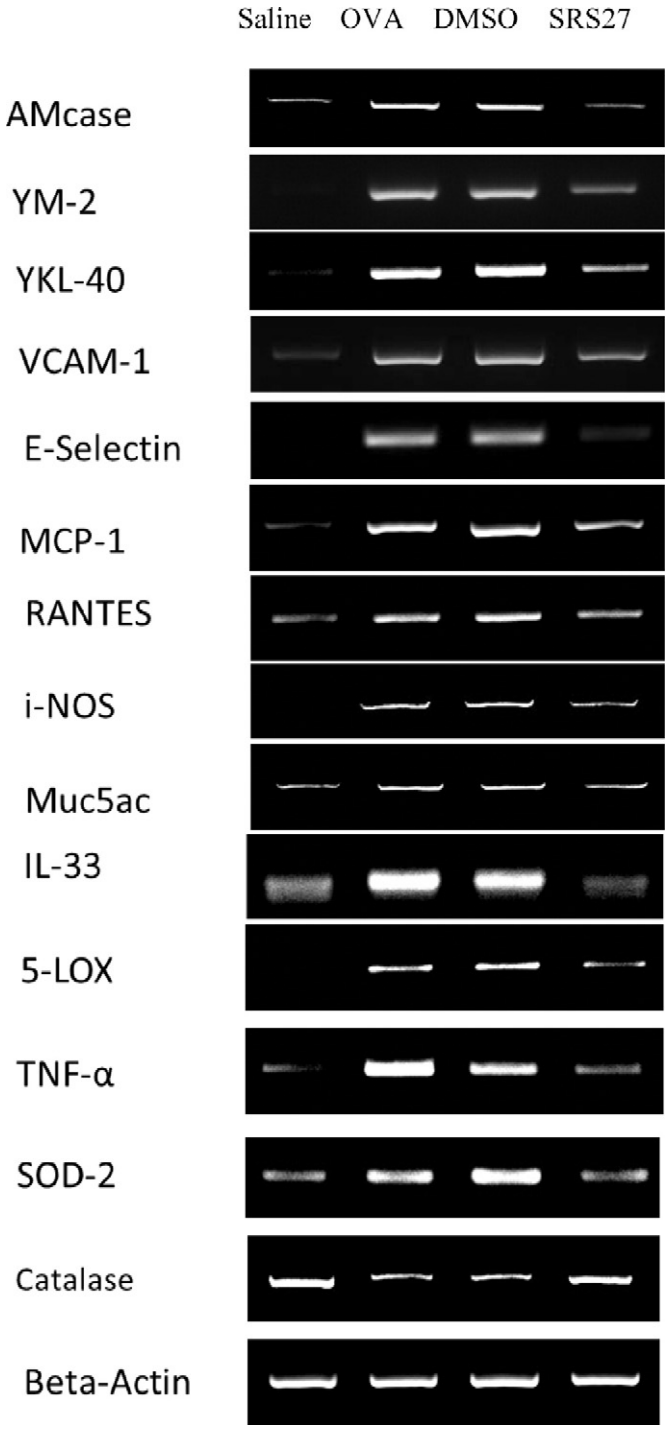


Fig. 7. Effects of SRS27 on ovalbumin-induced NF-κB activity and inflammatory gene expression in airway inflammation. (a) Representative images of polymerase chain reaction products of Saline = saline control mice, OVA = OVA-challenged mice, 3% DMSO = DMSO-treated mice, and 3.0 mg/kg SRS27 = 3.0 mg/kg SRS27-treated mice. Beta-actin was used as a loading control. Mean relative intensity of bands against saline group from three different lung samples with similar patterns observed were quantified using Image J. Gene expressions of AMCase, YM-2, YKL-40, VCAM-1, E-selectin, Muc5ac, 5-LOX, TNF-α, iNOS, IL-17, IL-33, CCL5, CCL2, catalase, and SOD-2 were significantly down-regulated by SRS27. Values shown are the mean ± SD (n = 3). *Significantly different from vehicle control (3% DMSO), $P < 0.05$. Take note that basal level of E-selectin was undetectable; as such fold increase of E-selectin is not displayed in the figure. (b) Representative images of immunoblotting of p65 level in lung nuclear protein lysate (Saline = saline control mice, OVA = OVA-challenged mice, 3% DMSO = DMSO-treated mice and SRS27 = 3.0 mg/kg SRS27-treated mice). TATA binding protein was used as a loading control. DMSO-treated lung samples were used as the vehicle control. Intensity of bands against saline group was quantified using Image J. SRS27 significantly reduced level of non-phosphorylated NF-κB p65 in lung tissue. Values shown are the mean ± SD (n = 3). *Significantly different from vehicle control (3% DMSO), $P < 0.05$. (c) Nuclear binding activity of NF-κB in lung tissue (Saline = saline control mice, OVA = OVA-challenged mice, 3% DMSO = DMSO-treated mice and SRS27 = 3.0 mg/kg SRS27-treated mice) determined using a TransAM™ p65 transcription factor ELISA kit. DMSO-treated lung samples were used as the vehicle control. SRS27 significantly reduced nuclear binding activity of NF-κB p65 in lung tissue. Values shown are the mean ± SEM (n = 3). *Significant difference from 3% DMSO in saline control, $P < 0.05$.

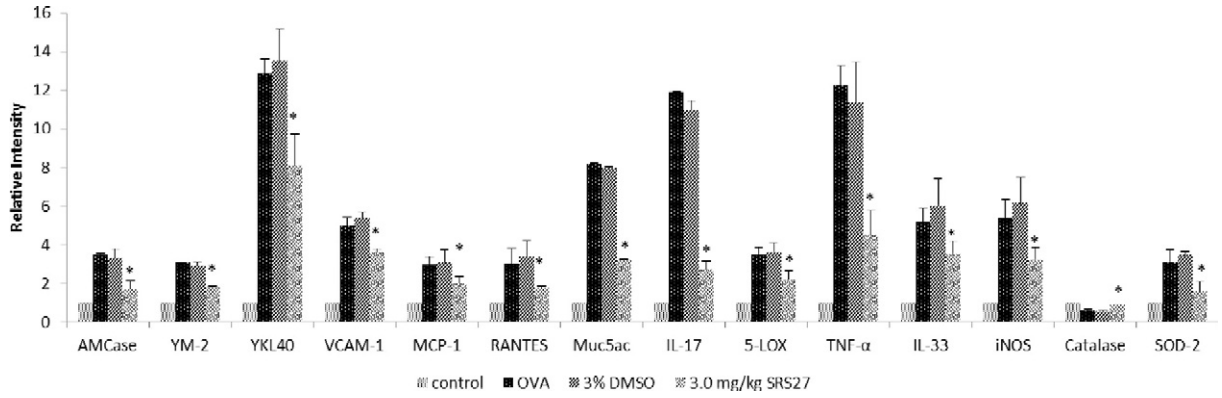


Fig. 7 (*continued*).

signalling cascades leading to NF-κB activation and production of lipid mediators, cytokines, and chemokines (Galli et al., 2008). Therefore, the observed reduction in serum total IgE and OVA-specific IgE by SRS27 in our OVA-mouse model of asthma may be attributed to its inhibitory effect on B-cell activation *via* inhibition of NF-κB activation, and its effect on IL-4 and IL-13 mediated class switching to IgE.

Airway inflammation and AHR development involve multiple inflammatory cells and mediators (Barnes, 2011). It has been established that IL-4 and IL-5 also play critical roles in AHR by mobilizing and activating eosinophils, leading to the release of pro-inflammatory products, such as major basic protein and cysteinyl leukotrienes, which are closely associated with AHR (Takatsu and Nakajima, 2008; Shifren et al., 2012). SRS27 significantly inhibited OVA-induced AHR by increasing concentrations of methacholine. Thus, the observed reduction of AHR by SRS27 may be associated with the reduction in Th2 cytokine production, tissue eosinophilia and serum IgE level.

Chitinase proteins such as AMCase, Ym1, Ym2, and YKL-40, have been found to increase in airway inflammation in human and mouse model of asthma and may play a role in airway remodeling. They are mainly expressed in airway epithelium and alveolar macrophages (Shuhui et al., 2009). Overall, chitinase may play a role in airway inflammation and remodeling. SRS27 markedly down-regulated AMCase, Ym2, and, YKL-40 mRNA expression in the lungs of OVA-challenged mice. The decrease might be caused by a decrease in IL-4 and IL-13 levels in the airways with SRS27 treatment and may contribute to the diminished pulmonary eosinophilia.

Oxidative stress is closely associated with other hallmarks such as airway inflammation, mucus secretion, and AHR (Wood and Gibson, 2010). In normal conditions, a healthy lung is protected from low levels of oxidative stress by anti-oxidants such as super oxide dismutase and catalase (Giustarini et al., 2009a); however, in asthma, exposure to allergens up-regulates the production of ROS and RNS such as superoxide anion, hydrogen peroxide, hydroxyl radical, and NO (Caramori and Papi, 2004). This is followed by the induction of a cascade of pro-inflammatory cytokines, chemokines, and adhesion molecules. Further increase in oxidative stress will ultimately inflict direct toxic effects, causing cellular apoptosis, necrosis and oxidative lung damage. Therapeutic approaches for reducing oxidative stress in a mouse model of asthma were proven effective by using the anti-malarial drug, artesunate (Ho et al., 2012). Clinical studies have shown a positive correlation of 8-isoprostane levels in exhaled breath condensates from asthmatics with the severity of asthma (Baraldi et al., 2003). On the other hand, 8-OHdG is an indicator of oxidative DNA damage (Giustarini et al., 2009b) and is elevated in severe asthmatics (Nadeem et al., 2003). SOD is responsible for the dismutation of ROS into less potent H_2O_2 and has been shown to be induced in airway inflammation (Nadeem et al., 2003). Catalase on the other hand, catalyzes the decomposition of H_2O_2 to water and oxygen (Nadeem et al., 2003) and the gene expression was noticeably reduced in OVA-challenged condition. In this study, 8-isoprostane, 8-OHdG and SOD were reduced whereas catalase was increased in SRS27-treated inflamed lungs, suggesting that SRS27 could markedly lessen ROS and RNS in the lungs and prevent oxidant-induced lung damage.

5. Conclusion

The effect of SRS27 on the OVA-mouse model of asthma had been proven as SRS27 was able to reduce OVA-induced inflammatory cell recruitment into BAL fluid, IL-4, IL-5 and IL-13 and CCL11 production, serum IgE synthesis, pulmonary eosinophilia, mucus hypersecretion, and AHR, possibly *via* the inhibition of NF-κB activity at the translocation level. With these promising pharmacological activities, this prototype chemical entity could be developed as a prophylactic treatment for asthma and potentially a new alternative to glucocorticosteroids. In addition, further studies to include therapeutic dosing regimen and direct delivery of the compound to the airway should be carried out to support the use for the treatment of asthma. Moreover, we speculate that other signalling pathways such as Wnt/β-catenin and 5-lipoxygenase pathways that are involved in inflammation could also be targets of SRS27. In summary, SRS27 is a first semisynthetic DDAG analogue tested to be an effective anti-asthmatic compound in the mouse model of asthma, possibly targeting the persistent NF-kB signalling pathway activation which leads to down-regulation of AHR and inflammatory parameters.

Supplementary data to this article can be found online at http://dx.doi.org/10.1016/j.taap.2016.04.004.

Author contributions

Participated in study conception and design: Sidik, Lajis, Stanslas, and Wong.

Participated in acquisition of data: Lim, Goh, Sagineedu, and Yong.

Participated in analysis and interpretation of data: Lim, Yong, Sidik, Lajis, Wong, and Stanslas.

Participated in drafting of manuscript: Lim and Sagineedu.

Participated in critical revision of the manuscript: Wong and Stanslas.

Statement of conflicts of interest

None.

Transparency document

The Transparency document associated with this article can be found, in the online version.

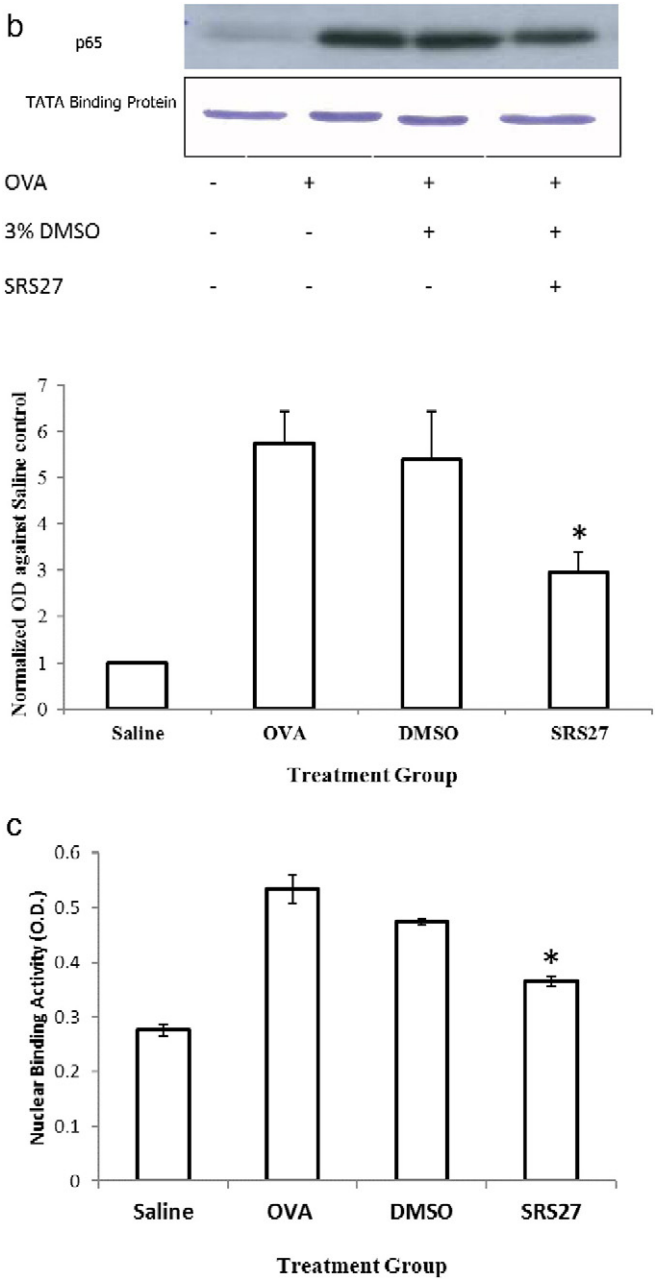


Fig. 7 (*continued*).

Acknowledgements

The authors' work reported herein was supported by a grant (BMRC/09/1/21/19/595) from the BioMedical Research Council of Singapore. Jonathan Lim Chee Woei would like to thank Universiti Putra Malaysia for the award of study leave and Ministry of Higher Education for Academic Training Scheme of Institute of Higher Education (SLAI) scholarship.

References

Aromdee, C., 2012. Modifications of andrographolide to increase some biological activities: a patent review (2006–2011). Expert Opin. Ther. Pat. 22, 169–180.

Bao, Z., Guan, S., Cheng, C., Wu, S., Wong, S.H., Kemeny, D.M., Leung, B.P., Wong, W.S., 2009. A novel antiinflammatory role for andrographolide in asthma via inhibition of the nuclear factor-kappaB pathway. Am. J. Respir. Crit. Care Med. 179, 657–665.

Baraldi, E., Carraro, S., Alinovi, R., Pesci, A., Ghiro, L., Bodini, A., Piacentini, G., Zacchello, F., Zanconato, S., 2003. Cysteinyl leukotrienes and 8-isoprostane in exhaled breath condensate of children with asthma exacerbations. Thorax 58, 505–509.

Barnes, P.J., 2008. The cytokine network in asthma and chronic obstructive pulmonary disease. J. Clin. Invest. 118, 3546–3556.

Barnes, P.J., 2011. Pathophysiology of allergic inflammation. Immunol. Rev. 242 (1), 31–50.

Bartlett, N.W., Slater, L., Glanville, N., Haas, J.J., Caramori, G., Casolari, P., Clarke, D.L., Message, S.D., Aniscenko, J., Kebadze, T., Zhu, J., Mallia, P., Mizgerd, J.P., Belvisi, M., Papi, A., Kotenko, S.V., Johnston, S.L., Edwards, M.R., 2012. Defining critical roles for NF-κB p65 and type I interferon in innate immunity to rhinovirus. EMBO Mol. Med. 4 (12), 1244–1260.

Brightling, C., Berry, M., Amrani, Y., 2008. Targeting TNF-α: a novel therapeutic approach for asthma. J. Allergy Clin. Immunol. 121, 5–10.

Bureau, F., Delhalle, S., Bonizzi, G., Fiévez, L., Dogné, S., Kirschvink, N., Vanderplasschen, A., Merville, M.P., Bours, V., Lekeux, P., 2000. Mechanisms of persistent NF-kappa B activity in the bronchi of an animal model of asthma. J. Immunol. 165 (10), 5822–5830.

Caramori, G., Papi, A., 2004. Oxidants and asthma. Thorax 59, 170–173.

Chao, W.W., Kuo, Y.H., Lin, B.F., 2010. Anti-inflammatory activity of new compounds from *Andrographis paniculata* by NF-kappaB transactivation inhibition. J. Agric. Food Chem. 58, 2505–2512.

Choi, I.W., Kim, D.K., Ko, H.M., Lee, H.K., 2004. Administration of antisense phosphorothioate oligonucleotide to the p65 subunit of NF-kappaB inhibits established asthmatic reaction in mice. Int. Immunopharmacol. 4, 1817–1828.

Ciriaco, M., Ventrice, P., Russo, G., Scicchitano, M., Mazzitello, G., Scicchitano, F., Russo, E., 2013. Corticosteroid-related central nervous system side effects. J. Pharmacol. Pharmacother. 4 (1), S94–S98.

Collart, M.A., Baeuerle, P., Vassalli, P., 1990. Regulation of tumor necrosis factor alpha transcription in macrophages: involvement of four kappa B-like motifs and of constitutive and inducible forms of NF-kappa B. Mol. Cell. Biol. 10, 1498–1506.

De Stefano, D., 2011. Oligonucleotides decoy to NF-kappaB: becoming a reality? Discov. Med. 12 (63), 97–105.

Desmet, C., Gosset, P., Pajak, B., Cataldo, D., Bentires-Alj, M., Lekeux, P., Bureau, F., 2004. Selective blockade of NF-kappa B activity in airway immune cells inhibits the effector phase of experimental asthma. J. Immunol. 173, 5766–5775.

Fujita, T., Fujitani, R., Takeda, Y., Takaishi, Y., Yamada, T., Kido, M., Miura, I., 1984. On the diterpenoids of *Andrographis paniculata*: X-ray crystallographic analysis of andrographolide and structure determination of new minor diterpenoids. Chem. Pharm. Bull. (Tokyo) 32, 2117–2125.

Galli, S.J., Grimbaldeston, M., Tsai, M., 2008. Immunomodulatory mast cells: negative, as well as positive, regulators of immunity. Nat. Rev. Immunol. 8, 478–486.

Gilmore, T.D., Herscovitch, M., 2006. Inhibitors of NF-kappaB signaling: 785 and counting. Oncogene 25 (51), 6887–6899.

Giustarini, D., Dalle-Donne, I., Milzani, A., Rossi, R., 2009a. Oxidative stress induces a reversible flux of cysteine from tissues to blood in vivo in the rat. FEBS J. 276, 4946–4958.

Giustarini, D., Dalle-Donne, I., Tsikas, D., Rossi, R., 2009b. Oxidative stress and human diseases: Origin, link, measurement, mechanisms, and biomarkers. Crit. Rev. Clin. Lab. Sci. 46 (5-6), 241–281.

Goh, F.Y., Upton, N., Guan, S.P., Cheng, C., Shanmugam, M.K., Sethi, G., Leung, B.P., Wong, W.S., 2012. Fisetin, a bioactive flavonol, attenuates allergic airway inflammation through negative regulation of NF-κB. Eur. J. Pharmacol. 679, 109–116.

Goto, K., Chiba, Y., Misawa, M., 2009. IL-13 induces translocation of NF-kappaB in cultured human bronchial smooth muscle cells. Cytokine 46, 96–99.

Guan, S.P., Kong, L.R., Cheng, C., Lim, J.C., Wong, W.S., 2011. Protective role of 14-deoxy-11,12-didehydroandrographolide, a noncytotoxic analogue of andrographolide, in allergic airway inflammation. J. Nat. Prod. 74, 1484–1490.

Hart, L.A., Krishnan, V.L., Adcock, I.M., Barnes, P.J., Chung, K.F., 1998. Activation and localization of transcription factor, nuclear factor-kappaB, in asthma. Am. J. Respir. Crit. Care Med. 158 (5), 1585–1592.

Hein, H., Schlüter, C., Kulke, R., Christophers, E., Schröder, J.M., Bartels, J., 1997. Genomic organization, sequence, and transcriptional regulation of the human eotaxin gene. Biochem. Biophys. Res. Commun. 237, 537–542.

Heinz, M., Lemke, P., Anagnostopoulos, I., Hacker, C., Krappmann, D., Mathas, S., Dörken, B., Zenke, M., Stein, H., Scheidereit, C., 2002. Nuclear factor kappaB-dependent gene expression profiling of Hodgkin's disease tumor cells, pathogenetic significance, and link to constitutive signal transducer and activator of transcription 5a activity. J. Exp. Med. 196, 605–617.

Ho, W.E., Cheng, C., Peh, H.Y., Xu, F., Tannenbaum, S.R., Ong, C.N., Wong, W.S., 2012. Anti-malarial drug artesunate ameliorates oxidative lung damage in experimental allergic asthma. Free Radic. Biol. Med. 53, 498–507.

Hogan, S.P., Rosenberg, H.F., Moqbel, R., Phipps, S., Foster, P.S., Lacy, P., Kay, A.B., Rothenberg, M.E., 2008. Eosinophils: biological properties and role in health and disease. Clin. Exp. Allergy 38 (5), 709–750.

Jada, S.R., Hamzah, A.S., Lajis, N.H., Saad, M.S., Stevens, M.F., Stanslas, J., 2006. Semisynthesis and cytotoxic activities of andrographolide analogues. J. Enzyme Inhib. Med. Chem. 21, 145–155.

Kato, A., Favoreto Jr., S., Avila, P.C., Schleimer, R.P., 2007. TLR3- and Th2 cytokine-dependent production of thymic stromal lymphopoietin in human airway epithelial cells. J. Immunol. 179 (2), 1080–1087.

Kim, H.Y., DeKruyff, R.H., Umetsu, D.T., 2010. The many paths to asthma: phenotype shaped by innate and adaptive immunity. Nat. Immunol. 11, 577–584.

Lemanske, R.F., Jr Busse, W.W., 2003. 6. Asthma. J. Allergy Clin. Immunol. 111, S502–S519.

Lim, J.C., Chan, T.K., Ng, D.S., Sagineedu, S.R., Stanslas, J., Wong, W.S., 2012. Andrographolide and its analogues: versatile bioactive molecules for combating inflammation and cancer. Clin. Exp. Pharmacol. Physiol. 39, 300–310.

Li-Weber, M., Krammer, P.H., 2003. Regulation of IL4 gene expression by T cells and therapeutic perspectives. Nat. Rev. Immunol. 3, 534–543.

Matsuda, T., Kuroyanagi, M., Sugiyama, S., Umehara, K., Ueno, A., Nishi, K., 1994. Cell differentiation-inducing diterpenes from *Andrographis paniculata* Nees. Chem. Pharm. Bull. (Tokyo) 42, 1216.

Matsumoto, K., Terakawa, M., Fukuda, S., Kato, A., Toki, S., Shinohara, M., Wakiguchi, H., Saito, H., 2006. CpG oligodeoxynucleotide prolongs eosinophil survival through activation of contaminating B cells and plasmacytoid dendritic cells in vitro. Int. Arch. Allergy Immunol. 140, 42–50.

Moriuchi, H., Moriuchi, M., Fauci, A.S., 1997. Nuclear factor-kappa B potently up-regulates the promoter activity of RANTES, a chemokine that blocks HIV infection. J. Immunol. 158, 3483–3491.

Nadeem, A., Chhabra, S.K., Masood, A., Raj, H.G., 2003. Increased oxidative stress and altered levels of antioxidants in asthma. J. Allergy Clin. Immunol. 111, 72–78.

Newton, R., Holden, N.S., Catley, M.C., Oyelusi, W., Leigh, R., Proud, D., Barnes, P.J., 2007. Repression of inflammatory gene expression in human pulmonary epithelial cells by small-molecule IkappaB kinase inhibitors. J. Pharmacol. Exp. Ther. 321, 734–742.

Pope, S.M., Zimmermann, N., Stringer, K.F., Karow, M.L., Rothenberg, M.E., 2005. The eotaxin chemokines and CCR3 are fundamental regulators of allergen-induced pulmonary eosinophilia. J. Immunol. 175 (8), 5341–5350.

Poynter, M.E., Cloots, R., van Woerkom, T., Butnor, K.J., Vacek, P., Taatjes, D.J., Irvin, C.G., Janssen-Heininger, Y.M., 2004. NF-kappa B activation in airways modulates allergic inflammation but not hyperresponsiveness. J. Immunol. 173 (11), 7003–7009.

Schindler, U., Baichwal, V.R., 1994. Three NF-kappa B binding sites in the human E-selectin gene required for maximal tumor necrosis factor alpha-induced expression. Mol. Cell. Biol. 14, 5820–5831.

Schulze-Luehrmann, J., Ghosh, S., 2006. Antigen-receptor signalling to nuclear factor kappa B. Immunity 25, 701–715.

Shifren, A., Witt, C., Christie, C., Castro, M., 2012. Mechanisms of remodeling in asthmatic airways. J. Allergy (Cairo) 2012, 316049.

Shuhui, L., Mok, Y.K., Wong, W.S., 2009. Role of mammalian chitinases in asthma. Int. Arch. Allergy Immunol. 149, 369–377.

Takatsu, K., Nakajima, H., 2008. IL-5 and eosinophilia. Curr. Opin. Immunol. 20, 288–294.

Vroling, A.B., Duinsbergen, D., Fokkens, W.J., van Drunen, C.M., 2007. Allergen induced gene expression of airway epithelial cells shows a possible role for TNF-α. Allergy 62, 1310–1319.

Wills-Karp, M., 2004. Interleukin-13 in asthma pathogenesis. Immunol. Rev. 202, 175–190.

Wood, L.G., Gibson, P.G., 2010. Reduced circulating antioxidant defences are associated with airway hyper-responsiveness, poor control and severe disease pattern in asthma. Br. J. Nutr. 103, 735–741.

Wood, L.G., Gibson, P.G., Garg, M.L., 2003. Biomarkers of lipid peroxidation, airway inflammation and asthma. Eur. Respir. J. 21, 177–186.

Xing, L., Remick, D.G., 2005. Mechanisms of dimethyl sulfoxide augmentation of IL-1 beta production. J. Immunol. 174 (10), 6195–6202.

Supplementary Figures

Figure S1a:

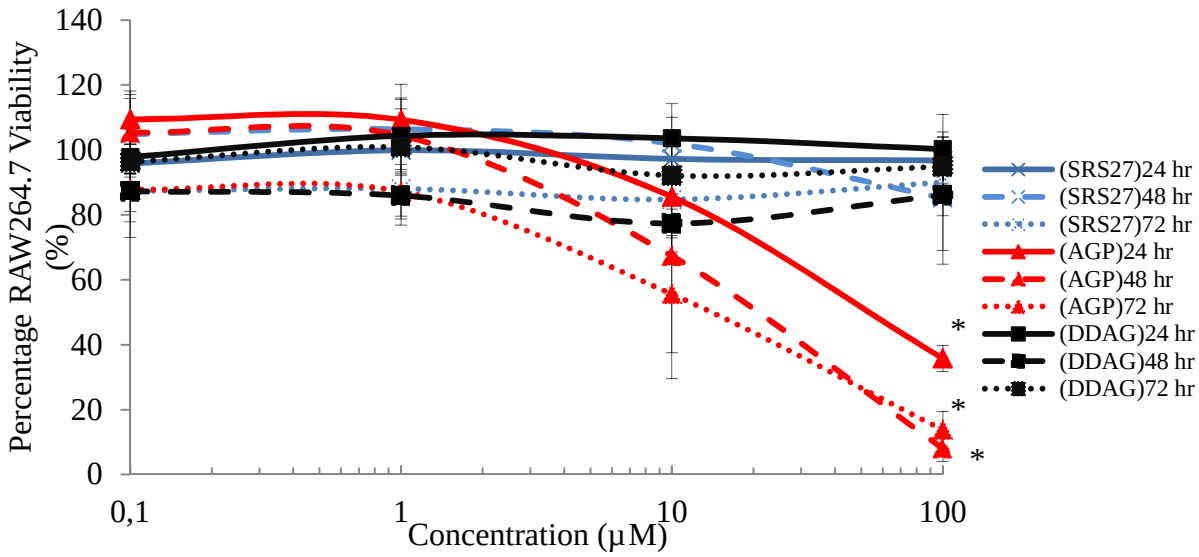


Figure S1b:

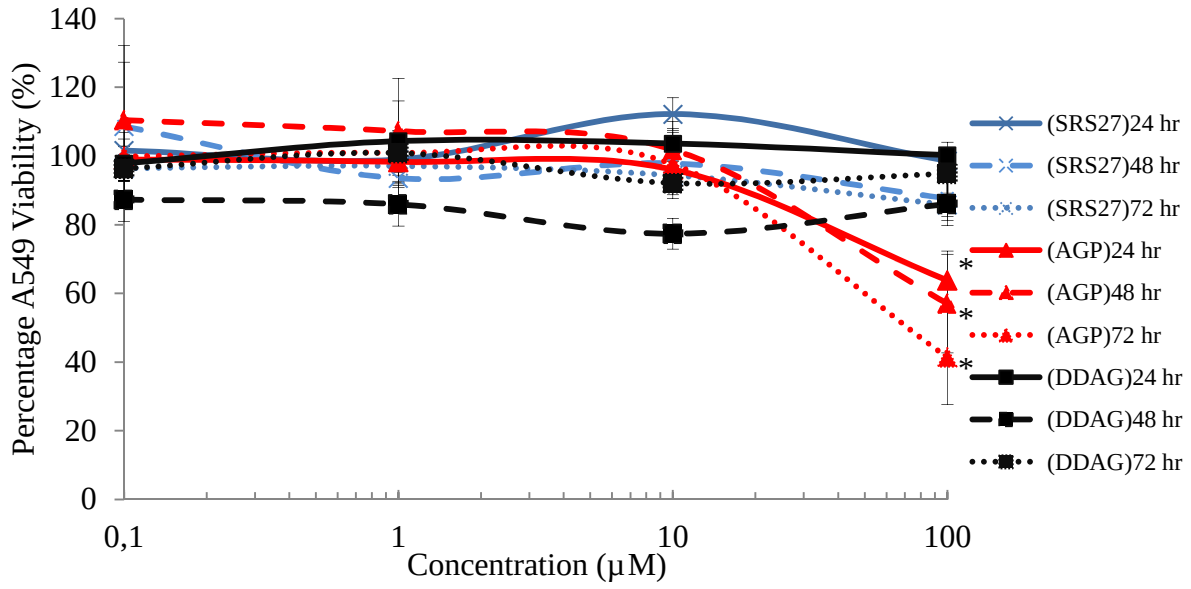


Figure S1c:

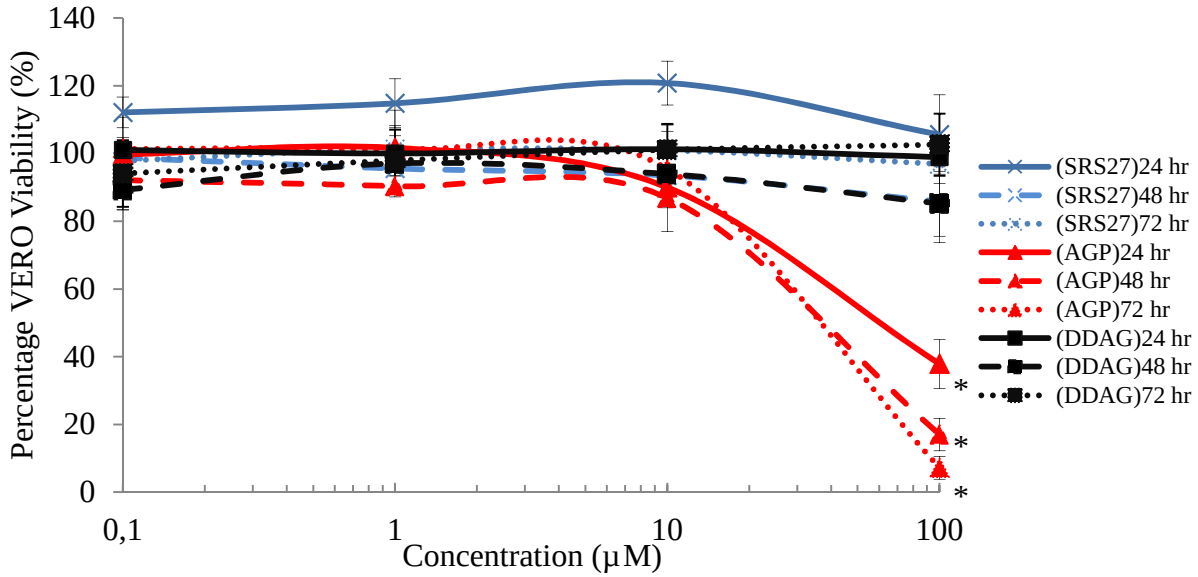


Figure S1: Dose-response cytotoxic effects of AGP, DDAG and SRS27 on the viability of RAW264.7 (A), (A549 (B), and VERO (C). Cells were exposed to compounds for 4 h followed by removal of compounds from the media. The cells were then incubated for 24, 48 and 72 h in compound free media. AGP displayed toxicity signs at range of 10-100µM whereas DDAG and SRS27 were not toxic towards of all tested cell lines. Values represent relative percentage of mean viability of cells as compared with control ± S.D. (n= 3). *p< 0.05.

Figure S2a:

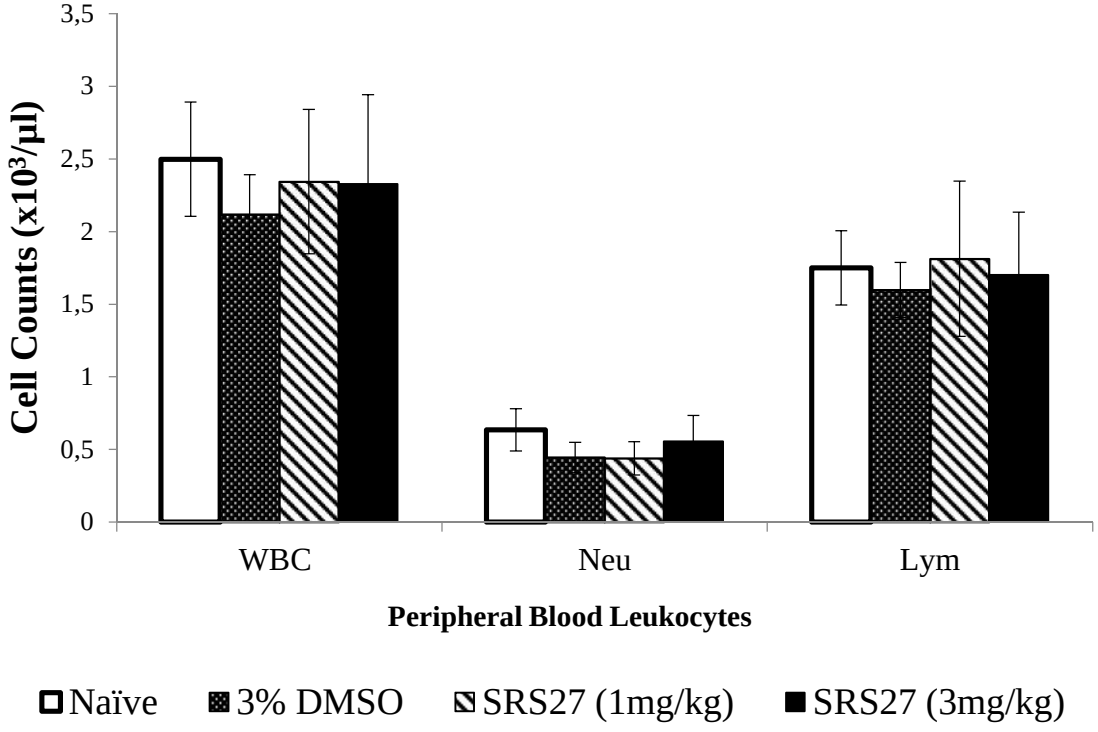


Figure S2b:

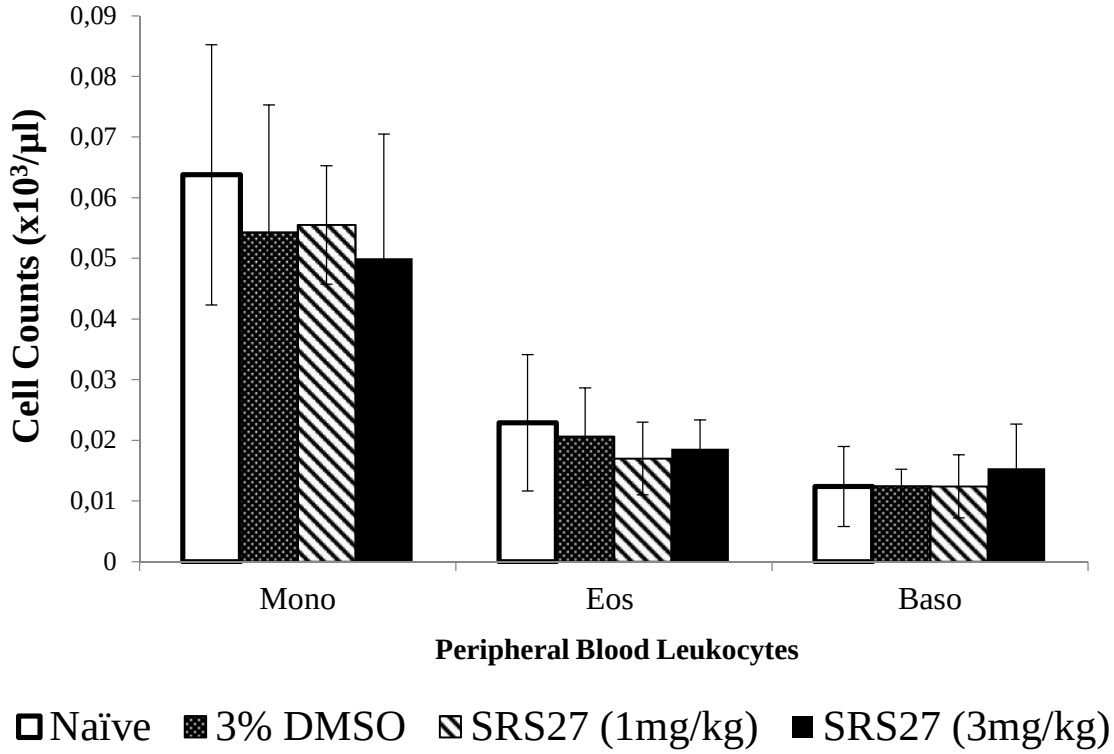


Figure S2: Peripheral blood leukocytes analysis of haematological blood profile obtained from saline-challenged (Naïve), vehicle control (3% DMSO), and SRS27-treated asthmatic

BALB/C mice. WBC= total white blood cells, Neu= neutrophil, Lym= lymphocyte, Mono= monocyte, Eos= eosinophil, Baso= basophil. Peripheral blood leukocytes of 1 and 3 mg/kg of SRS27 treatment groups did not significantly fluctuate from those of naïve mice. Values are expressed as mean ± SD (n= 6).

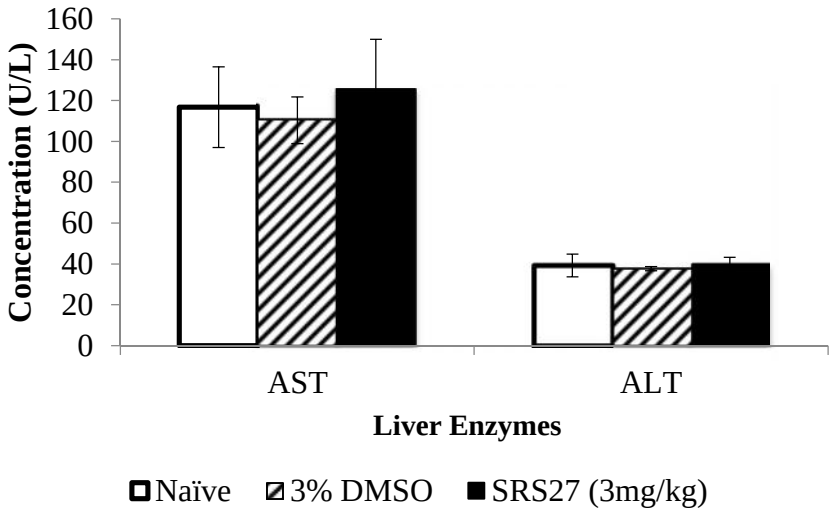


Figure S3: AST and ALT level in serum of saline-challenged (Naïve), vehicle control (3% DMSO) and asthmatic mice treated with 3 mg/kg of SRS27 measured during the toxicity study. SRS27 at 3 mg/kg did not adversely affect liver function. Values are expressed as mean ± SD (n= 6).

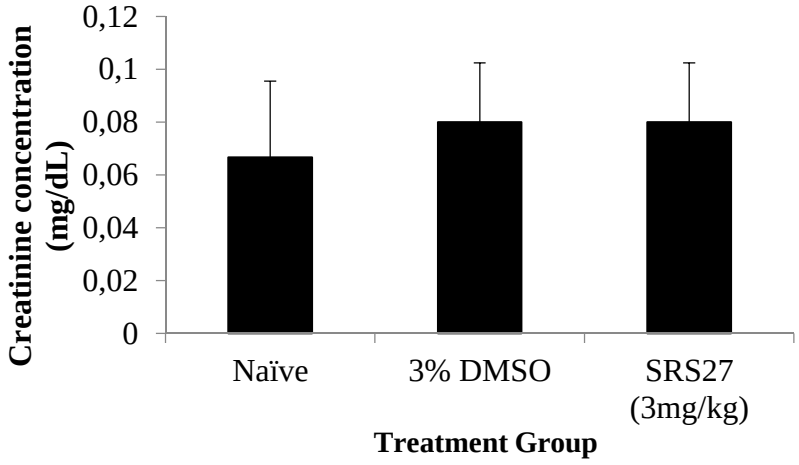


Figure S4: Creatinine level in serum of control (Naïve), vehicle control (3% DMSO) and mice treated with 3 mg/kg of SRS27. SRS27 at 3 mg/kg did not adversely affect kidney function. Values are expressed as mean ± SD (n= 6).

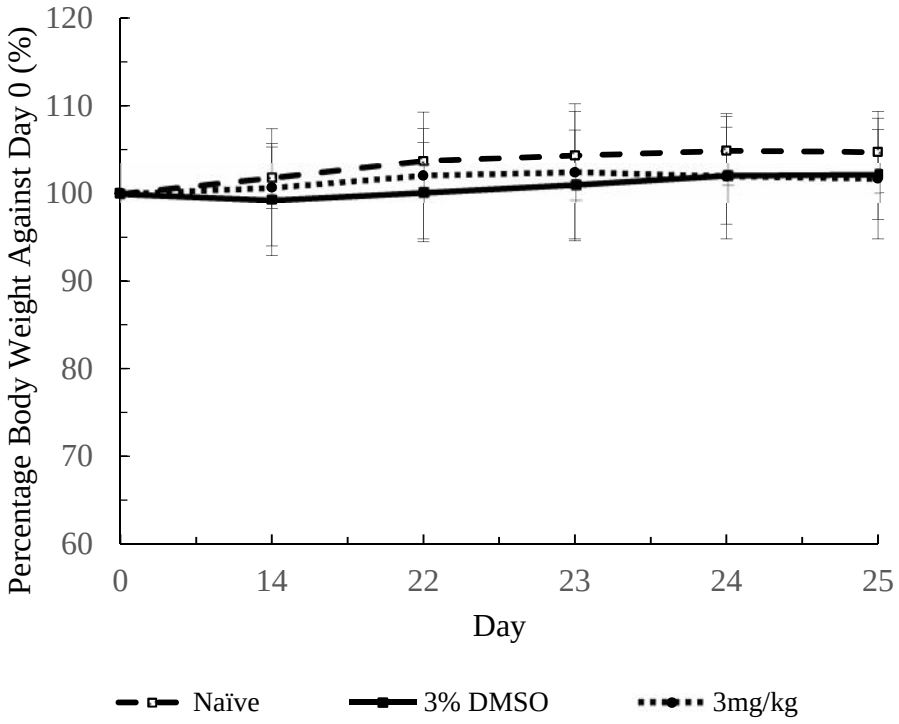


Figure S5: Percentage normalised body weight changes relative to day 0 of control (Naïve), vehicle control (3% DMSO) and mice treated with 3 mg/kg of SRS27. No significant body weight change in all treatment groups in comparison to naïve group from day 0 to day 25. Values are expressed as mean ± SD (n= 6).

Tables

Table S1: Primers for inflammatory biomarkers

Targets	Primer Sequences
iNOS	Forward 5'- CGGGCAAACATCACATTCAGATCCCG-3' Reverse 5'- TATATTGCTGTGGCTCCCATGTT -3'
Muc5ac	Forward 5'-GAGGGCCCAGTGAGCATCTCC-3' Reverse 5'-TGGGACAGCAGCAGTATTCAGT-3'
CCL5	Forward 5′-CATATGGCTCGGACACCA-3′ Reverse 5′-ACACACTTGGCGGTTCCT-3′
CCL2	Forward 5'-CTTCTGGGCCTGCTGTTCA-3' Reverse 5'-CCAGCCTACTCATTGGGATC-3'
IL-17	Forward 5'-CCGCAATGAAGACCCTGATAGA-3' Reverse 5'-CAGCATCTTCTCGACCCTGAAA-3'
IL-33	Forward 5'-GATGGGAAGAAGGTGATGGGTG-3' Reverse 5'-TTGTGAAGGACGAAGAAGGC-3'

Catalase	Forward 5'-ACCAGGGCATCAAAAACTTG343-3' Reverse 5'-GCCCTGAAGCTTTTTGTCAG-3'
SOD2	Forward 5'-ACCAGTGCAGGACCTCATTTTAA-3' Reverse 5'- TCTCCAACATGCCTCTCTTCATC-3'
TNF-α	Forward 5'-GACGTGGAAGTGGCAGAAGAG-3' Reverse 5'-TGCCACAAGCAGGAATGAGA-3'
5-Lox	Forward 5'-CACGGGGACTACATCGAGTT-3' Reverse 5′-AAC CTCACATGGGCTACCAG-3'
Catalase	Forward 5'-ACCAGGGCATCAAAAACTTG343-3' Reverse 5'-GCCCTGAAGCTTTTTGTCAG-3'
SOD2	Forward 5'-ACCAGTGCAGGACCTCATTTTAA-3' Reverse 5'- TCTCCAACATGCCTCTCTTCATC-3'
TNF-α	Forward 5'-GACGTGGAAGTGGCAGAAGAG-3' Reverse 5'-TGCCACAAGCAGGAATGAGA-3'
5-Lox	Forward 5'-CACGGGGACTACATCGAGTT-3' Reverse 5′-AAC CTCACATGGGCTACCAG-3'
AMCase	Forward 5'-TGGGTTCTGGGCCTACTATG-3' Reverse5'-GCTTGACAATGCTGCTGGTA-3'
Ym-2	Forward 5'-CAGAACCGTCAGACATTCATTA-3' Reverse 5'-ATGGTCCTTCCAGTAGGTAATA-3'
Ykl-40	Forward 5'-GTACAAGCTGGTCTGCTACT-3' Reverse 5'-GTTGGAGGCAATCTCGGAAA-3'
VCAM-1	Forward 5'-CAAGGGTGACCAGCTCATGAA-3' Reverse 5'-TGTGCAGCCACCTGAGATCC-3'
E-Selectin	Forward 5'-AACGCCAGAACAACAATTCC-3' Reverse 5'-TGAATTGCCACCAGATGTGT-3'
IL-6 (human)	Forward 5'-CAGGAGAAGATTCCAAAGAT-3' Reverse 5'-ACTGGTTCTGTGCCTGCAGC-3'
IL-8 (human)	Forward 5'-ATGACTTCCAAGCTGGCCGTGGCT-3' Reverse 5'-CTCAGCCCTCTTCAAAAACTTCTC-3'
CCL5 (human)	Forward 5'-ATGAAGGTCTCCGCGGCACGCCT-3' Reverse 5-CTAGCTCATCTCCAAAGAGTTG-3'
CCL2 (human)	Forward 5'-GATCTCAGTGCAGAGGCTCG-3' Reverse 5'-TGCTTGTCCAGGTGGTCCAT-3'
β-Actin	Forward 5'-TCATGAAGTGTGACGTTGACATCCGT-3' Reverse 5'-CCTAGAAGCATTTGCGGTGCACGATG-3'

Table S3: ^{1}H NMR spectral data for compounds DDAG and SRS27; δ (ppm); multiplicity (J in Hz)

^{1}H	**^{1}H NMR**	
	DDAG	**SRS27**
3	3.49 (1H, dd, *J* = 11.5, 4.0)	4.57 (1H, m)

9	2.33 (1H, d, *J* = 10.0)	2.32 (1H, d, *J* = 10.2)
11	6.89 (1H, dd, *J* = 15.5, 10.0)	6.90 (1H, dd, *J* = 15.6, 10.2)
12	6.13 (1H, d, *J* = 15.5)	6.11 (1H, d, *J* = 15.6)
14	7.19 (1H, br s)	7.15 (1H, br s)
15	4.81[a]	4.79 (1H, br s)
17	4.81[a]	4.79 (1H, br s)
	4.55 (1H, s)	4.57 (1H, m)
18	1.28 (3H, s)	1.01 (3H, s)
19	4.28 (1H, d, *J* = 11.0)	4.36 (1H, d, *J* = 12.0)
	4.15 (1H, d, *J* = 11.0)	4.13 (1H, d, *J* = 12.0)
20	0.83 (3H, s)	0.88 (3H, s)
3-OCOC**H$_3$**	-	2.03 (3H, s)
19-OCOC**H$_3$**	-	2.01 (3H, s)

[a] Obscured by overlapping with other signals.

Table S4: ^{13}C NMR spectral data for DDAG and SRS27; δ (ppm)

Carbon	**^{13}C NMR**	
	DDAG	**SRS27**
1	38.49	38.51
2	28.20	24.39
3	81.00	80.28
4	43.16	41.60
5	54.93	55.02
6	23.21	24.11

7	36.80	36.98
8	148.33	148.11
9	61.89	61.97
10	38.79	36.87
11	136.23	135.85
12	121.30	121.60
13	129.51	129.43
14	143.17	143.37
15	69.87	69.78
16	172.57	172.37
17	109.36	109.49
18	22.89	22.92
19	64.41	-
20	16.11	15.47
3-O**C**OCH$_3$	-	171.08
3-OCO**C**H$_3$	-	21.39
19-O**C**OCH$_3$	-	171.23
19-OCO**C**H$_3$	-	21.28

87

88